bioRxiv preprint doi: https://doi.org/10.1101/2021.10.15.464493; this version posted October 16, 2021. The copyright holder for this preprint (which was not certified by peer review) is the author/funder. All rights reserved. No reuse allowed without permission.

Propionate ameliorates diabetes-induced neurological dysfunction through regulating the PI3K-AKT-eNOS signaling pathway

Qin Wu[2†], Jiajun Dong[2†], Yahong Cheng[1]*, Gaofeng Jiang[3]*

[1]Key Laboratory of Combinatorial Biosynthesis and Drug Discovery, Ministry of Education, Wuhan University School of Pharmaceutical Sciences, Wuhan University, Wuhan, Hubei, P. R. China

[2]Zhejiang University-University of Edinburgh Institute, Zhejiang University, Hangzhou, Zhejiang, P. R. China

[3]Center for Translational Medicine, Tianyou Hospital, Wuhan University of Science and Technology, Wuhan, Hubei, P. R. China

 Corresponding authors

E-mail address: yahongcheng@whu.edu.cn (Yahong Cheng); jianggf@wust.edu.cn (Gaofeng Jiang);

Phone: +86-18627009067

[†] These authors contributed to the work equally and should be regarded as co-first authors.

Abstract

Diabetes-entailed disorder of cognition, deemed as "diabetes-entailed brain malfunction", finds its confirmation from numerous literature. Current evidence supports that oxidative stress, neuronal apoptosis, and cerebral microcirculation weakness are associated with cognition deficits induced by diabetes. The present study explores the effect of propionate on neurological deficits, cerebral blood flow, and oxidative stress in diabetic mice. Propionate could markedly improve neurological function, which was correlated with its capabilities of stimulating NO production, increasing cerebral microcirculation, suppressing oxidative stress and reducing neuron loss in the hippocampus. In addition, the results of western blotting indicated that the brain-protective function of propionate in STZ-induced T1DM mice is related to PI3K/AKT/eNOS signaling pathway. To sum up, cure by using ester or salt of propionic acid weakens brain-related blood circulation in the microvascular system, programmed cell death of the hippocampus and nerve-related malfunction based on a mouse-modeled diabetic disease. Thus, ester or salt of propionic acid, utilized for preserving comestible at present, is potentially advantageous to the amelioration of cognition-related decay entailed by diabetic disease.

Highlights

- Propionate ameliorates diabetic-induced depression-like behavior, spatial learning and memory deficits.
- Propionate increases cerebral microcirculation by enhancing NO production in diabetic mice.
- Propionate suppresses oxidative stress and reduces neuron loss in the hippocampus.
- Brain protective function of propionate is related to PI3K/AKT/eNOS signaling pathway.

Graphical Abstract

bioRxiv preprint doi: https://doi.org/10.1101/2021.10.15.464493; this version posted October 16, 2021. The copyright holder for this preprint (which was not certified by peer review) is the author/funder. All rights reserved. No reuse allowed without permission.

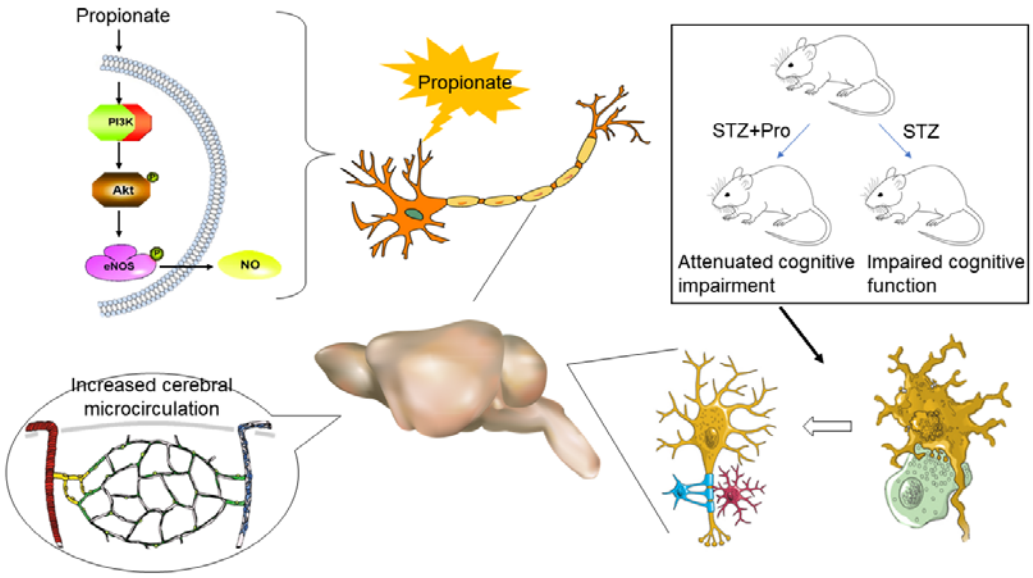

Keywords: Propionate; T1DM; Cerebral microcirculation; Neurological dysfunction; PI3K-AKT-eNOS signaling pathway

Abbreviations: **T1DM,** type one diabetes mellitus; **DM,** diabetes mellitus; **STZ**, streptozocin; **NO**, nitric oxide; **ROS**, reactive oxygen species; **SOD**, superoxide dismutase; **CAT**, catalase; **MDA**, Malondialdehyde; **LCBF,** local cerebral blood flow; **CNS**, central nervous system; **TST,** tail suspension test; **FST,** force swimming test; **MWM**, Morris water maze; **EPM**, elevated plus-maze

1. Introduction

Cognitive disorder is very common among diabetic patients. Clinical research shows that both type 1 and type 2 diabetes patients are always accompanied by varying degrees of neurological dysfunction [1, 2], the incidence of which is related to the course of the disease, the selection of hypoglycemic drugs and other factors [3]. Slight cognitive impairment may occur in mild cases, and dementia may develop in severe cases [4]. Therefore, to find effective drugs for the prevention and treatment of diabetic learning nerve function impairment is a research hotspot in this field. Dietary supplementation with nutrients that protect brain tissue from damage may be a promising treatment approach for neurological complications caused by diabetes.

Propionic acid is a kind of short chain fatty acid (SCFA), which is usually added to cheese, bread, animal feed and artificial spices as a preservative [5], and the concentration of propionic acid added as a food additive ranges from 1.0-2.5g/kg. It is reported that propionate plays an important biological role by acting as an antioxidant, anti-inflammatory, antiviral, anti-cancer, etc [6-8]. Some studies have shown that propionate can inhibit lipid synthesis in rat hepatocytes [9]. When the concentration of propionic acid was 0.1mmol/L, the synthesis of 50% cholesterol and triglyceride was inhibited [10]. In addition to reducing cholesterol and fat production, propionate may also be involved in weight control by suppressing appetite [11]. In a human research, ester or salt of propionic acid dramatically provoked the discharge of PYY as well as GLP-1 out of human-colon cells. Acute intake of 10 g plant polysaccharide propionate-ester dramatically augmented after-meal plasma PYY as well as GLP-1. Besides, it lessened energy uptake [11].

In addition to its role in peripheral nerves, more and more evidence indicate that propionic acid may play an important role in the central nervous system (CNS) [11]. Propionic acid was

bioRxiv preprint doi: https://doi.org/10.1101/2021.10.15.464493; this version posted October 16, 2021. The copyright holder for this preprint (which was not certified by peer review) is the author/funder. All rights reserved. No reuse allowed without permission.

found to enter the brain from the bloodstream in a concentration-dependent manner [12]. Propionic acid is catalyzed to propionyl CoA by thiokinase. Then propionyl CoA reacts with carbon dioxide to generate methylmalonyl CoA under the catalysis of propionyl CoA carboxylase. Finally, methylmalonyl CoA is catalyzed to succinyl CoA by the mutase, thus participating in the tricarboxylic acid cycle and ATP synthesis which provides energy for the brain [13].

However, the therapeutic effect and underpinning mechanisms of propionate on treating diabetes-related neurological complications have not been studied yet. Although the pathologic mechanisms of diabetes-induced nervous system impairment are not fully understood, an increasing number of studies have illustrated that decreased angiogenesis induced by oxidative stress is associated with neurological dysfunction [14-16]. Oxidative stress is the most essential pathologic factor in the early phase [17]. Oxygen radical damages endothelial cells and induce their apoptosis, which greatly restricts the angiogenesis in brain tissue and limits the blood supply to the brain tissue [18-20]. It also impacts the secretion of neurotrophic factors by endothelial cells, which exhibit a repair effect to the function of impaired neurons [21]. Therefore, it will be a novel and effective therapeutic strategy for treating diabetic neurological complications to prevent oxidative stress injury and thus protect endothelial cells and promote angiogenesis.

Excitatory amino acid toxicity, immune inflammatory reaction, free radicals and nitric oxide damage are the main factors leading to neuron apoptosis [22]. Recently, phosphoinositide 3-kinase (PI3K)/serine-threonine protein kinase (Akt) signaling pathway has attracted much attention due to its regulatory role in neuronal apoptosis [23, 24]. PI3K, the activation of which is realized via sensing organ of chemotaxis provoker, has been suggested as a signal-giving enzyme. Activating PI3K generates the second message-giving inherent-protein 3 of the semi-permeable limiting layer of cell protoplasm, combining with signal-giving protein AKT as well as phosphoinositide-dependent kinase-1 (PDK1). The integration entails the chemical or enzymic introduction into a compound of a phosphoryl group of Ser308 in AKT by PDK1, activating AKT, a key downstream-effect generator of PI3K [25]. Phosphorylation of Akt and nitric oxide synthetase is an essential pathway of NO synthesis in endothelial cells [26-28]. However, whether the intervention of propionate is capable of influencing PI3K/Akt/eNOS signaling pathway is unclear.

The effect of propionate in animal models with diabetic-induced neuronal dysfunction needs to be explored. Therefore, the present study focuses on evaluating the effect of propionate on blood glucose level and neuronal function in streptozocin (STZ)-induced diabetic mice. The effect of propionate on cerebral blood flow, oxidative stress, neuronal apoptosis, and PI3K-Akt-eNOS signaling pathway were evaluated at the cellular or protein level through approaches including basic pathological tests, biochemical tests, enzyme-linked immunosorbent assays, and western blot. This study provides not only a theoretical and experimental foundation on propionate effect of alleviating diabetes-related neurological complications, but also a novel economical, effective and side-effect-free candidate compound for the treatment of diabetic patients with a neurological disorder.

2. Materials and methods

2.1. Reagents and Chemicals

Sodium propionate, being pure over 99% purity, were produced by Sinopharm Chemical Reagents Co., Ltd (Wuhan, China). Streptozotocin (STZ) as well as metformin were bought from Sigma-Aldrich (St. Louis, Mo, USA). The dissolving of STZ was done by citrate buffing solvent

bioRxiv preprint doi: https://doi.org/10.1101/2021.10.15.464493; this version posted October 16, 2021. The copyright holder for this preprint (which was not certified by peer review) is the author/funder. All rights reserved. No reuse allowed without permission.

whereas the one of sodium propionate as well as metformin were done via distillate water.

2.2. Animals

Sixty male Kunming adult mice weighted 18 to 22 grams were used. Every five mice shared one cage and all mice had free access to food and water, under a 12-hour light/12-hour dark condition. Mice were cared strictly compliant with the guidance of the National Institutes of Health Guide for the Care and Use for Laboratory Animals and all animal experiments were performed with the approval of the Institutional Animal Care and Used Committee of Wuhan University. Animals were administered treatments in a randomized double blind design, and treatments were randomized across cages to avoid cage level effects.

2.3. Experiment-inducting of diabetes as well as plan of cures

Diabetic disease was provoked by STZ (35mg/kg, i.p.) arranged in citrate-buffing solvent (pH 4.4, 0.1M) and the control-mice got same amount of citrate-buffing solvent. Blood-glucose level was decided by glucometer seven days later of injecting STZ. Mice with empty-stomach plasma-glucose levels over 11.1mmol/L were chosen for deeper research. Upon the confirmation of diabetes, divided teams of mice (N=10 for each group) has by oral the application of sodium propionate (37.5, 75 or 150 mg/kg), metformin (100 mg/kg), or vehicle (0.1 ml/10 g distillate-water in place) one time a day (9:00 a.m.) for thirty six days consecutively. Illustration 1 suggests the experiment plan.

The amount of ester or salt of propionic acid in comestible such as bread is from 1.0 to 2.5 g each kilogram. And the dose of propionate used in the present study was determined based on the dose applied as a food preservative. The amount limit of ester or salt of propionic acid was judged per our initial researches, revealing at time that the amount limit of ester or salt of propionic acid was less than 37.5 mg/kg, it was invalid. Nevertheless, at time that the amount limit of ester or salt of propionic acid was over 75 mg/kg, it might become hard for creatures to ingest. Given this, we set up high-, middle-, and low-dosage series to survey the effectiveness of anti-diabetic disease of the 3 different amount of doses.

2.4. Blood glucose and glucose tolerance test

Before the experiment, mice were fasted for 16 hours. Blood was obtained by drawing blood from a vein which is 2 mm from the distal end of the tail and baseline glucose levels were assessed using a glucometer. Mice were intraperitoneally injected with 100 mg/ml glucose solution in sterile water at 2 g/kg body weight. After 0, 30, 60, 120 minutes after the sugar was given, the blood was taken again to measure glucose levels.

2.5. Body weight recording

All the experimental mice were weighed at 14:00 to 15:00 once per 3 days throughout the experiment.

2.6. Nissl staining

To evaluate the change of neuronal numbers, Nissl staining was performed. Mice were euthanized (N=6 per group) and perfused with 0.9% NaCl solution and 4% paraformaldehyde solution for brain fixation. The entire brain was then isolated and further fixated in paraformaldehyde for more than 24 hours. The brain was embedded in paraffin and sliced into 5 μm thick coronal sections. Paraffin sections were dewaxed and rehydrated before being stained with toluidine blue. Three sections were randomly selected from each mouse, and the stained sections were observed and photographed under a light microscope (Nikon, Tokyo, Japan) in the CA3 region of the hippocampus area. The number of neurons in this region was counted at high magnification (200×)

bioRxiv preprint doi: https://doi.org/10.1101/2021.10.15.464493; this version posted October 16, 2021. The copyright holder for this preprint (which was not certified by peer review) is the author/funder. All rights reserved. No reuse allowed without permission.

[29].

2.7. Cerebral blood flow measurement

A moorFLPI-2 Full-Field Laser Perfusion Imager (Moor Instruments, Axminster, UK) was utilized to measure local cerebral blood flow. Anesthesia was induced with 4% chloral hydrate, following which mice (N=5 per group) were fixed on a stereotaxic frame plate with a constant temperature of 37□. An incision of skin was made to expose the skull surface, where ultrasound gel was applied. LCBF was conducted for 5 min, 25 Hz for sampling frequency and 1 s per frame. The data images were analyzed with moorFLPI2 Full-Field Laser Perfusion Imager Review v5.0 software. For each animal, brain ROI was drawn, and ROI flux data was obtained from 19 images per scan. The mean value was used for subsequent analysis. All the analysis was blinded to experimental conditions [30].

2.8. Determination of oxidative stress-related indicators

2.8.1. Measurement of CAT, SOD and MDA

Upon the completion of the behaviour-based tests, mice (n = 4) euthanization was started, following tissue-extracting out of the cerebral hippocampus area, after which the tissue (10 %, w/v) homogenization was started quickly via potassium-phosphate buffing agent (pH 7.4) below 0° Celsius before the tissue centrifuging with 3000 rpm, under the temperature of 4 □ and lasting 10 minutes. The entailed overlying materials were amassed and utilized for analyzing biochemicals.

Protein content was quantified with a commercially available BCA protein assay kit (Solarbio Science and Technology Co., Beijing, China). Malondialdehyde (MDA) level, as a marker of lipid peroxidation, was assessed as contents of thiobarbituric acid-reactive substances (TBARS) by spectrophotometry; the level of superoxide dismutase (SOD) was determined by xanthine oxidase method as the index of the antioxidant system (Nanjing Jiancheng Bioengineering Institute). Based on the operation instruction, catalase (CAT) determination was performed by using a commercial CAT assay kit (Nanjing Jiancheng Bioengineering Institute) [31].

2.8.2. Detection of ROS level

Mouse ROS ELISA kit was used to determine ROS concentration. The hippocampal tissues of mice (N=5 per group) were extracted, homogenized, centrifuged and the supernatant was collected. 40μl supernatant was added to 96-well plate and reagents were applied according to manufacturer's instruction. The absorbance of the mixture at 450 nm was determined by a microplate analyzer. The standard curve was obtained by plotting the concentration of the standard solution with the corresponding absorbance. The sample concentration was determined based on the absorbance of the sample to be tested and expressed as U/mgprot.

2.9. Assessment of NO level

The overlying materials of hippocampus homogenized substances was utilized for the measurement of NO level. NO level was assessed for the purpose of evaluating endothelial cell function in the brain vasculature of diabetic mice. In the body or in an aqueous solution, NO is extremely easy to be oxidized into NO^{2-}. Low acidic pH value promotes the reaction of NO^{2-} with diazosalt amine sulfonate to form diazo compound, which further couples with naphthalene vinyl diamine to form a product is characterized by an absorption peak of 550 nm. The level of NO can be determined by measuring the absorption value. The NO concentration in brain tissue was determined using a NO assay kit and following the instruction of the manufacture's (Caozhiyuan Biotechnology Co., Ltd.).

bioRxiv preprint doi: https://doi.org/10.1101/2021.10.15.464493; this version posted October 16, 2021. The copyright holder for this preprint (which was not certified by peer review) is the author/funder. All rights reserved. No reuse allowed without permission.

2.10. Western blotting

Western blotting was performed following a standard protocol. 20 μg of protein sample from the hippocampus per lane was separated through sodium dodecyl sulfate-polyacrylamide gel electrophoresis (SDS-PAGE). The proteins in the gel were subsequently transferred onto polyvinylidene fluoride (PVDF) membranes and then immunological visualized. Primary antibodies of anti-PI3K (1:1000), anti-p-PI3K (1:5000), anti-AKT (1:1000), and anti-p-AKT (1:5000) were used. β-actin (1:5000) was used as an internal reference. The membrane was incubated overnight at 4 □, and the chemiluminescence signal of interest was visualized using an imager (BIO-RAD Gel Doc XR, America) [32].

2.11. Functional tests

Preceding studies showed that behavioral malfunctions, for example, the depressive disorder as well as dyskinesia occurred in TIDM mice after inducing STZ. In this study, animals were rotated through each test on different days. The testing time order was kept unchanged for the guarantee of the identical testing circumstances of all animals. The conducting of all tests was done blindly. In addition, the observing personnel had no idea of the cures that the mice have been granted.

2.11.1. Open field test

A black open-field apparatus (50 × 50 × 40 cm, with 25 equal squares) made of lacrylic box was used to assess the exploratory willingness and spontaneous locomotor activity. The center of the arenas was defined as the central nine squares. Mice (N=10 per group) were placed individually into the center area and allowed 5-min free behave. Animal behavior was recorded using a video tracking system and was analyzed automatically using OFT-100 software. Total distance traveled, the time spent in the center and quiescent, and rearing times were calculated. The apparatus was cleaned with 70% alcohol and dried between trials [33].

2.11.2. Tail suspension test

A tail suspension test (TST) was performed to evaluate the depression index of animals by observing the time of immobility and agitation [34]. The instrument for this test is a grey acrylic box (54 cm height) with an open front and a metallic hook at the top. We use laboratory sticky tape to hang mice (N=10 per group) by the tails from the hook. Their movements were captured for 6 minutes via a camera complete with tracking software. The total immobility period and climbing times were calculated by using the event count mode of RWD software. Longer immobility time was an indicator of depression [35].

2.11.3. Forced swimming test

The FST was performed for the purpose of determining behavior related to depression [36]. Each mouse was placed alone in a vertical plexiglass cylinder (140 mm in diameter, 200 mm high) that contained water at a depth of 150 mm and a temperature of 23-25°C, for a period of 8 min. Recorded for the same period, a blinded experimenter scored each mouse's immobility time for the last 6 min. Immobility was recognized when a mouse was floating and moving a minimal amount to keep its head and body from becoming submerged. The researcher remained in the room for the duration of the test, and the water was changed between the introduction of each new mouse to prevent odors (N=10 per group) [37].

2.11.4 Elevated plus maze test

The elevated plus-maze test is to investigate the anxiety state of animals by using the contradictory behaviors of exploration and the fear of the high position. The EPM has a pair of open arms (28.5×7cm) and two closed arms (28.5×7×14 cm) they are separated by a central

bioRxiv preprint doi: https://doi.org/10.1101/2021.10.15.464493; this version posted October 16, 2021. The copyright holder for this preprint (which was not certified by peer review) is the author/funder. All rights reserved. No reuse allowed without permission.

platform (7cm×7cm). The apparatus is 50 cm high. Each mouse was placed on the central platform. The number of entries is recorded, and the time spent in the open arm is recorded over a 5 min time session (N=10 per group).

2.11.5. Morris water maze task

MWM was performed to test the spatial learning and memory of the animals. The basic device of the water maze is a circular pool with a diameter of 1.2 meters and a height of 0.6 meters. The water inside is colored milky white with non-fat milk powder. The water temperature in the pool was maintained at 25±1□.

The pool was evenly divided into four quadrants (called south, east, north, west), an invisible platform with a diameter of 8 cm was hidden 1 cm below the water surface in the target quadrant. The whole test contains 2 phases, navigation test and probe test. During the navigation phase, mice (N=10 per group) were released into the pool from randomly assigned release points, one trial lasted 60 s at most, ~~the~~ and ~~mice~~ would be guided to the platform beyond the time limit and allowed to stay for 15 s. Four trials were run for the MWM navigation phase every day and these were conducted on days 1− 4. The operating venue was canceled out of the pool on day 5. Besides, probe experiments happened. During the probe phase, the platform was removed from the pool, mice were released for 1 min to swim freely. Tracks of mice in the pool were recorded with the Smart3.0 software during the training and probe phase. Besides, recording and analysis of the time consumed in the initial operating venue quadrant (targeted quadrant), the quantity of operating venue crossings as well as travel-velocity under the 60-s-interval were done [38].

2.12. Statistical analysis

All statistics were analyzed using SPSS statistics version 25, and graphs were generated by Prism 6.0 (GraphPad Software, Inc.). Data for the GTT, body weight and escape latencies in the MWM test were analyzed with a two-way analysis of variance (ANOVA). Measuring information of the rest outcomes were beside single-directed variance analyzing (ANOVA). Arithmetic mean ± SD was used to indicate statistical differences, where p less 0.05 was considered statistically significant.

3. Results

3.1. Reduction of fasting blood glucose and improvement of glucose intolerance by propionate treatment

Sixteen hours later of the stoppage of food taking, the fasting blood-glucose (FBG) of mice with diabetes augmented dramatically ($p<0.001$). However, propionate (75 mg/kg) and metformin (100 mg/kg) treatments significantly decreased FBG ($p<0.001$) and there was no significant difference among the low dose, middle dose and STZ groups (Fig. 2A). Regarding the intraperitoneal-glucose tolerating test (IPGTT), via the calculation of the area under the curve (AUC) of blood-glucose, the AUC of the STZ group was observed dramatically above the one of the Ctrl-group ($p<0.001$) (Illustration 2B-C; Table 1). Comparing with STZ administrated group, propionate administration reduced the AUC ($p<0.05$ in 37.5 and 150 mg/kg groups; $p<0.001$ in 75 mg/kg group), and treatment of 75 mg/kg propionate has significant advantages over 37.5 mg/kg and 150 mg/kg of propionate gavage groups. The data clearly showed administration of propionate at a dose of 75 mg/kg effectively decreased the FBG and improved glucose intolerance in T1D mice. In the remaining experiments, propionate at a dose of 75 mg/kg was selected for intervention.

3.2. Propionate ameliorated STZ-induced body weight loss

bioRxiv preprint doi: https://doi.org/10.1101/2021.10.15.464493; this version posted October 16, 2021. The copyright holder for this preprint (which was not certified by peer review) is the author/funder. All rights reserved. No reuse allowed without permission.

The normal control group exhibited a gradual increase in body weight from 19.9±2.50g to 43.8±3.25g. (Fig. 3). Meanwhile, the streptozotocin-induced mice exhibited a significant decrease in body weight from 20.3±3.27g to 33.1±4.28g ($p<0.001$) in comparison to the former group. Conversely, when compared to the model group, the animals who received propionate ($p<0.001$) or metformin ($p<0.01$) exhibited a significant enhancement in their body weight, from 20.3±2.81g to 40.2±2.94g and from 19.2±1.28g to 37.4±1.62g, respectively. The outcomes suggested streptozotocin is effective for cutting the body weight dramatically in the creatures where it was applied, beside the control group in particular; at the same time, their body weight showed a obvious augmentation after cure with ester or salt of propionic acid, helping curbing the weight decrease entailed by the streptozotocin.

3.3. Improvement of LCBF by propionate intervention

We determined the effects of propionate and metformin on the local cerebral blood flow (LCBF) of mice since LCBF levels can provide objective indicators for cerebral circulation or obstruction. LCBF was measured by Doppler flowmetry (Fig. 4). The STZ-administrated group exhibited a compromised LCBF level with approximately 35.11% decrement ($p<0.001$). The pre-treatment of propionate significantly increased LCBF comparing with the model group ($p<0.01$); while metformin treatment failed to reverse LCBF decrement caused by STZ. These observations indicated that propionate could rescue decreased LCBF levels induced by diabetes.

3.4. Oxidative stress partially ameliorated by pretreated propionate

3.4.1. Propionate enhanced CAT and SOD levels

The effect of propionate on antioxidase was further studied by measuring CAT and SOD activities. As Fig. 5A showed, CAT activity was significantly reduced after STZ intervention when compared to the non-treated group ($p<0.01$). While CAT activity was significantly increased after propionate treatments compared with the STZ group ($p<0.01$). Furthermore, CAT in the propionate treated group was found to be higher than in metformin-treated group ($p<0.05$). In addition, SOD activity was obviously decreased in STZ-exposed mice in comparison to the control group ($p<0.01$). The activity of SOD was restored in mice following propionate or metformin treatment ($p<0.05$), and no substantial difference between the metformin and propionate groups was found (Fig. 5B).

3.4.2. Inhibition of MDA and ROS accumulation by propionate

To ascertained the potential anti-oxidative effect of propionate, we also measured MDA (a marker of lipid peroxidation) and ROS content in mice hippocampal tissue. The MDA contents in mice hippocampus are shown in Fig. 5C. MDA formation was detected to be significantly elevated in the STZ group compared to the control group ($p<0.001$). In contrast, significant decreases in MDA levels were found in propionate or metformin treatment groups comparing to the STZ group ($p<0.01$). No statistical difference was presented between propionate and metformin groups.

The effects of increased production of reactive oxygen species (ROS) involve brain damage. ROS can produce membrane damage, change inner proteins, induce lipids denaturation, and damage DNA. ROS concentration was detected in mice brain tissues. Mice administrated by STZ showed significantly higher ROS levels than the control group ($p<0.01$). ROS concentration was remarkably reversed by propionate intaking compared with the STZ group ($p<0.01$). While metformin treatments showed little benefit effects. Propionate application had a distinct advantage over metformin administration in reducing ROS concentration ($p<0.05$). In summary, propionate showed positive effects in scavenging excessive reactive oxygen levels in mice brains.

bioRxiv preprint doi: https://doi.org/10.1101/2021.10.15.464493; this version posted October 16, 2021. The copyright holder for this preprint (which was not certified by peer review) is the author/funder. All rights reserved. No reuse allowed without permission.

3.5. Propionate enhanced ATP levels

The amount of ATP in the modeled group was notably less compared with the controlled group ($p < 0.05$). After the treatment in advance by using ester or salt of propionic acid, it was efficiently augmented beside STZ-entailed group. Nevertheless, the ATP amount wasn't altered by metformin dramatically (Fig. 6A).

3.6. Enhancement of nitric oxide (NO) release by propionate therapy

We examed brain NO level to evaluate NO production in brain vasculature. NO concentration was significantly lower in the STZ group ($p<0.001$): less than two-thirds that of the control group (Fig. 6B). Pretreatment of propionate or metformin to the STZ-exposed mice raised NO levels by 59.2% and 31.5%, respectively compared with the STZ group ($p<0.001$ and $p<0.01$, respectively). The NO level in the propionate group was also elevated in comparison with that in the metformin group ($p<0.05$). The increased NO concentration indicated an effect of propionate to promote angiogenesis in the brain, with a significantly higher efficacy than metformin.

3.6. Administration of propionate rescues STZ-induced neuronal loss in the hippocampus

Thirty six days after STZ administration, we utilized Nissl staining to evaluate the structures of the hippocampus in each group through comparing the number of neurons in optical fields of the CA3 regions across different groups. STZ administration induced obvious lesions in neurons in the CA3 and caused significant neuronal degeneration ($p<0.001$). On the contrary, metformin and propionate rescued the degradation as demonstrated by the results that numbers of neurons in STZ + Pro and STZ + Met groups are significantly higher than that in the STZ group ($p<0.001$). Noteworthily, propionate exhibited a superior effect than metformin ($p<0.01$). The data indicated that pre-treatment of propionate could persistently alleviate neuronal necrosis resulted from STZ-induction.

3.7. Improvement of exploratory and locomotor activity following propionate administration

It is well documented that exploratory willingness and spontaneous locomotor activity can be assessed by the open field tests via measuring distance moved, number of rearing, and time duration in the center and immobility time. Here, we firstly found that propionate administration was able to reverse reduced distance traveled, number of rearing, and time spent at the center of the open field ($p<0.05$) caused by STZ treatments ($p<0.05$) (Fig. 8A, B and C). No statistical significance was presented on these three indexes between propionate and metformin groups. The immobility time was shown in Fig. 8D. Mice in the STZ group spent more immobility time than those in the control group ($p<0.001$). Nevertheless, propionate reversed this result ($p<0.001$). Notably, propionate-treated mice presented remarkably less immobility time than metformin-administrated mice ($p<0.05$). Therefore, the results from open field tests suggested that propionate could enhance the exploratory willingness of STZ-induced diabetic mice.

3.8. Antidepressant effects of propionate treatment

Next, these results were further confined in an elevated plus maze, which is wildly utilized to investigate the anxiety state of animals. As illustrated in Fig. 8, mice treated with STZ were less inclined to enter or remain in open arms ($p<0.01$ and $p<0.05$, respectively). However, propionate-treated or metformin-treated mice entered open arms more frequently than those in the STZ group (Fig. 9A, $p<0.05$). In addition, the retention time in open arms was significantly longer in the propionate-treated group than STZ model group ($p<0.05$). Interestingly, mice in the propionate group tarried for a longer period in open arms than mice in the metformin group ($p<0.05$). By contrast, metformin-treated mice showed no significant difference in time in open

bioRxiv preprint doi: https://doi.org/10.1101/2021.10.15.464493; this version posted October 16, 2021. The copyright holder for this preprint (which was not certified by peer review) is the author/funder. All rights reserved. No reuse allowed without permission.

arms with those in the STZ group (Fig. 9B). Thus, the results in open arm tests indicated that propionate treatment attenuated anxiety in the STZ-induced DM model.

Moreover, the effects of propionate on ameliorating mice's depression-like behaviors were estimated in tail suspension tests and forced swimming tests. As shown in Fig. 10A, STZ-induced diabetic mice presented significantly longer immobility time when suspended by tails ($p<0.05$). Both propionate and metformin diminished the immobility time ($p<0.05$ and $p<0.01$, respectively). STZ exposure reduced the intention of tail climbs (Fig. 10B, $p<0.001$), while propionate or metformin treatments significantly reversed these tendencies ($p<0.001$ and $p<0.05$, respectively). Interestingly, propionate showed a better effect in increasing tail climbing behaviors than metformin ($p<0.05$). Furthermore, mice in the STZ-treated model group showed a remarkable increase in immobility time than mice in the control group in forced swimming tests (Fig. 10C, $p<0.05$), which was significantly reduced with the presence of propionate or metformin administrations ($p<0.05$), although the immobility time in STZ + Pro group was still longer than STZ + Met group ($p<0.05$). Therefore, the results implied that the administration of propionate could ameliorate the depression-related status of mice induced by STZ induction.

3.9. Improvement of learning and memory by propionate

Spatial memory functions of mice were commonly evaluated by water maze tests. As shown in Fig. 11A and Table 2, we found a significantly longer escape latency of the STZ group than the control group on day 2 and day 3-4 ($p<0.05$ and $p<0.001$, respectively), although not on day 1. Compared with the STZ model group, propionate treatment significantly reduced the escape latency of mice on day 2-4 ($p<0.01$ on day 2 and 3; $p<0.001$ on day 4). Metformin also decreased the latency on day 2 ($p<0.001$) and day 4 ($p<0.05$) but the propionate group shown a significantly shorter latency time than the metformin group in the last two days ($p<0.05$ for day 3 and $p<0.01$ for day 4). In summary, both propionate and metformin could positively alter spatial learning of diabetic mice, while propionate was found to have better efficiency.

The number of crossing into the former location of the platform was also recorded (Fig. 12A). The STZ treated group showed a significant decrease in crossing number in comparison with the control group ($p<0.05$). Both metformin treatment and propionate treatment significantly restored the crossing number ($p<0.05$). Another indicator, time spent in the target quadrant in probe task, was significantly lower in STZ treated group in comparison to the control group ($p<0.01$) (Fig. 12B). While both the propionate-treated mice and metformin-treated mice spent a significantly longer time in the target quadrant than the STZ group ($p<0.001$ and $p<0.01$, respectively). Besides, the time that propionate-treated mice spent was longer than the metformin-treated group ($p<0.05$). As for the swimming velocity, there had been a falling-off in STZ treated group ($p<0.05$) (Fig. 12C). In contrast, the propionate-treated mice were faster ($p<0.05$), while the metformin-treated mice showed no significant acceleration compared to the propionate pretreated mice.

3.10. Potent activation of the PI3K/AKT/eNOS pathway by propionate

Propionate activates the PI3K/AKT/eNOS pathway in the hippocampus of diabetic mice. Western blotting was implemented in this study for the purpose of identifying the relative expression of phosphorylated PI3K, AKT, and eNOS. From the panel, the protein levels of PI3K, AKT and eNOS remained unaltered acrossing all 4 groups. While, the STZ significantly reduced the phosphorylation levels of PI3K, AKT and eNOS. Both metformin and propionate presented rescue effects on phosphorylation level of PI3K, AKT and eNOS comparing with the STZ group ($p<0.001$ for PI3K and AKT; $p<0.05$ for eNOS). Propionate had exserted stronger effects on

bioRxiv preprint doi: https://doi.org/10.1101/2021.10.15.464493; this version posted October 16, 2021. The copyright holder for this preprint (which was not certified by peer review) is the author/funder. All rights reserved. No reuse allowed without permission.

restoring phosphorylation levels of PI3K and AKT from the comparison between the propionate group and metformin group ($p<0.05$).

Discussion

Diabetes mellitus is the most common chronic metabolic syndrome is characterized by insulin deficiency or relative deficiency. The major symptom is chronic hyperglycemia caused by disturbance of saccharides, lipid, and protein metabolism [39]. According to an epidemiological survey in 2015, approximately 8% of the global population aged between 20 to 79 are suffered from diabetes, and the proportion is anticipated to rise to 9.9%. Abundant studies consistently suggest that DM affects the nervous system. Due to the prolonged life expectancy of DM patients, cognitive impairment and dementia have become new striking complications of DM [40] . DM-induced cognitive deficits are also known as diabetic encephalopathy [41] . Presently, many studies on diabetic encephalopathy worldwide focus on peripheral neuropathy, while the pathophysiological mechanisms of neuropathy caused by diabetic encephalopathy are less explored. However, with the significant increase of life expectancy of DM patients, the prevalence of diabetic cognitive dysfunction is bound to increase. Thus, illuminating the pathogenesis of diabetic cognitive dysfunction and seeking effective protective or therapeutic strategies are urgently required.

This study contributes to this research field by discovering the therapeutic effect of propionate on DM, which has not been discussed previously. Firstly, we noticed that propionate intervention decreased blood glucose levels in STZ-induced type I diabetic mice, reversed their weight loss, increased their local cerebral blood flow, and indirectly improved their neural function. Secondly, propionate showed good antioxidant activity and could alleviate the loss of neurons in the hippocampus in T1DM mice. Moreover, we discovered that the neural protective function of propionate may be associated with the modulation of NO biosynthesis and improved blood supply to brain tissues. Furthermore, we found that the brain-protective function of propionate in STZ-induced T1DM mice was related or at least partly related to PI3K/AKT/eNOS signaling pathway.

STZ is a broad-spectrum antibiotic. It has properties of antibacterial, antitumor, and causing diabetes, and it has high-selective toxicity of pancreatic β-cells in experimental animals. Its activity in inducing diabetes may be through free radical damage to islet β-cells, which impairs the insulin-producing function of islet β-cells and leads to diabetes. Intraperitoneal injection of STZ has recently been applied in many diabetes-related studies to specifically destroy pancreatic β-cells, resulting in secretion disorder and persistent hyperglycemia without toxicity to brain cells [42] . In this study, after a single intraperitoneal injection of STZ at 55 mg/kg to mice, their body weight was significantly decreased, and the fasting blood glucose level could reach up to or more than 20 mmol/L. Mice treated with STZ were generally in poor conditions, and some of them died before the terminal of the study.

Being the top extensively stipulated cure for sufferers with excess sugar in the blood, even for sufferers in paediatric department [43, 44], metformin is under the classification of biguanides as well as functions for decreasing blood glucose by reducing hepatic gluconeogenesis as well as enhancing insulin sensitiveness. Though having been utilized for treating diabetic disease for more than 6 decades, metformin, a clinically approved drug, has been found possible recently by evidences to be re-targeted for various other diseases, for example cancerous disease,

bioRxiv preprint doi: https://doi.org/10.1101/2021.10.15.464493; this version posted October 16, 2021. The copyright holder for this preprint (which was not certified by peer review) is the author/funder. All rights reserved. No reuse allowed without permission.

cardiovascular-related malfunctions, neurodegenerating related illnesses [45] as well as in more recent days, neuro-developmental malfunctions featured on the basis of intellectual-related retardation [46, 47]. The clarification of the functioning system of the metformin hasn't been entirely done. The metabolizing of energy serves as an exact critical element of metformin functioning. In addition, the latest proof shows its latent capacity for therapy might stem from the capability targeting mitochondria-related malfunction [48]. Cure done chronically by using metformin actually enhances mitochondria functioning capacity as well as strengths oxidation resistor protection. According with the capacity of metformin to transit the blood-brain protectie screen, these cure efficiencies received certification based on evidences not only in the peripheral area but also in the brain [49]. Thus, metformin was used as a positive control drug in this study.

Insufficient insulin secretion leads to hyperglycemia. Persistent high blood glucose may cause thickening of capillary basement membrane and narrowing of vessel lumen [50]. In combination with increased blood viscosity and slowed blood flow caused by metabolic disturbance of saccharides and lipids in diabetic patients, the structure changes of capillaries would decrease cerebral blood flow [51]. Some research has proved that the decrease of cerebral blood flow could cause dysfunction of the brain in information processing, manipulating, and integrating [52]. It would also impact cognitive response and processing ability, and eventually lead to impairment in learning and memory. In this study, cerebral blood flow was measured, besides the body weight and blood glucose level of mice. According to the results, in STZ-induced diabetic mice, their blood glucose level was markedly increased, and body weight was significantly decrease related to the control mice 36 days after STZ induction. As expected, results from cerebral blood flow studies also demonstrated obvious lower blood flow in high-glucose mice (36 days after STZ administration) than control mice. In contrast, after sodium propionate treatment, the blood glucose level of STZ-induced T1DM mice was significantly reduced. The sodium propionate exhibited the best effect on controlling blood glucose with a dose of 75 mg/kg. The weight gain of mice in the sodium propionate group was improved compared with the simple model group, moreover, the cerebral blood flow of the diabetic mice was significantly increased after 36 days compared with the model mice, as showed by results from cerebral blood flow measurement.

Studies have found that long-term hyperglycemia is closely related to diabetic neurological complications, and diabetic models have exhibited varying degrees of behavioral and cognitive dysfunction [53]. In this study, the behavior of experimental mice was evaluated by animal ethology methods, in order to study the improvement brought by propionate in neural function. The open-field test was used to evaluate the activity and exploration desire of mice, the tail suspension test and forced swimming test was used to evaluate the depression-like behaviors, and the water maze test was used to detect spatial learning and memory ability of mice. Experimental results showed that long-term hyperglycemia-induced significant cognitive and behavioral impairments, which are concretely showed in depression, a decline of learning and memory, and the results were consistent with that of previous studies about cognitive and behavioral impairments in diabetic models [54].

It has been reported that high glucose leads to excessive production of reactive oxygen species (ROS) in vascular endothelial cells [55]. Excessive ROS formation affects the hypoxia signaling pathway and further aggravates vascular endothelial disorders [56]. It causes damage to lipids,

bioRxiv preprint doi: https://doi.org/10.1101/2021.10.15.464493; this version posted October 16, 2021. The copyright holder for this preprint (which was not certified by peer review) is the author/funder. All rights reserved. No reuse allowed without permission.

proteins and mitochondrial DNA on the mitochondrial intima of neurons, resulting in intracellular energy failures and diabetic brain injury. At the same time, oxidative stress will result in metabolic disorders. The results of this study showed that the hippocampus CA3 area of the experimental diabetes model mice was significantly damaged, and the neuron loss was severe. The SOD and CAT activities in the brain tissue were significantly decreased, while the MDA content increased. The preventive intervention of propionate can significantly ameliorate the morphological changes of brain tissue and reduce the loss of neurons in the hippocampus, and antioxidant effects were also significantly enhanced. These findings indicate that propionate has a significant anti-oxidative function and can relieve hyperglycemia-induced brain damage in mice while promoting the regeneration of neurons.

Studies have shown that vascular endothelial cells can secrete a variety of vasoactive substances, including vasodilator factor NO. As a previous study suggested, NO synthesis is inhibited due to impaired vascular endothelial function in diabetic patients. Hyperglycemic environment leads to a reduction in endothelial cell function and reduction in the bioavailability of NO. In addition, high blood sugar culture conditions will accelerate the senescence of vascular endothelial cells, leading to impaired proliferation46. This study found that the NO level of model mice was significantly reduced, and propionate treatment significantly increased the NO level of mice. It is suggested that the therapeutic effect of propionate may be related to the regulation of NO synthesis and secretion. Other researches have found that inhibition of the PI3K/AKT/eNOS signaling pathway can engender vascular endothelial cell dysfunction, and a decrease in NO synthesis is observed when eNOS activity decreases since the eNOS is mainly activated by the PI3K/AKT signaling pathway. In this study, propionate treatment was shown to significantly upregulate the expression levels of PI3K/AKT/eNOS signaling pathway-related proteins, suggesting that propionate's brain protection function in STZ-induced type I diabetic mice is associated with PI3K/AKT/eNOS signaling pathway activation.

Our outcomes showed propionate (75 mg/kg) is able to serve positively for mice with damaged brains. Thus, about 0.5 g propionate shall be provided for someone weighing 60 kilograms via converting dosage from mice to human. The amount of propionate in bread ranges from 1.0 to 2.5 g each kilogram. We presume it is not hard to obtain the dose of propionate via food supplying. Supplementary elements in food taking with propionate included promises a bright future for the defense of brains from harm in T1DM. Even so, regarding the disparity between human and mice, the experimentation and efficiency of high-dosage propionate in various creature models of epileptic disease requires stricter researches prior to conducting clinical trials.

Conclusion

Taken together, strong evidence has been provided that propionate acts to ameliorate cerebral microcirculation to improve the cognitive abilities in diabetic mice, which may be attributed to its anti-diabetic, antioxidant and modulated by PI3K/Akt/eNOS pathway. The results of this study emphasize the importance of propionate on NO release, cerebral circulation, oxidative stress, and PI3K/Akt/eNOS pathway against high glucose insult.

Funding source

This study did not get any funding from funding agencies

Conflict of interest

The authors acknowledge no conflict of interest pertaining to the publication of the manuscript.

Acknowledgments

bioRxiv preprint doi: https://doi.org/10.1101/2021.10.15.464493; this version posted October 16, 2021. The copyright holder for this preprint (which was not certified by peer review) is the author/funder. All rights reserved. No reuse allowed without permission.

Thanks Shiqi Fan and Jinjin Li for their help in preparing samples and in measuring biochemical indices.

Author contributions

Yahong Cheng: Conceptualization, Writing-original draft and Writing-review & editing.

Yuan Jiang and Xinying Bai: Data curation and Methodology.

Qin Wu and Jiajun Dong: Software, Data curation, Methodology and Writing-original draft.

Gaofeng Jiang: Supervision, Validation and Methodology.

bioRxiv preprint doi: https://doi.org/10.1101/2021.10.15.464493; this version posted October 16, 2021. The copyright holder for this preprint (which was not certified by peer review) is the author/funder. All rights reserved. No reuse allowed without permission.

References

[1] A. Moheet, S. Mangia, E.R. Seaquist, Impact of diabetes on cognitive function and brain structure, Ann N Y Acad Sci 1353 (2015) 60-71.

[2] G.J. Biessels, S. Staekenborg, E. Brunner, C. Brayne, P. Scheltens, Risk of dementia in diabetes mellitus: a systematic review, The Lancet Neurology 5(1) (2006) 64-74.

[3] G. Barbara, B. Megarbane, L. Argaud, G. Louis, N. Lerolle, F. Schneider, S. Gaudry, N. Barbarot, A. Jamet, H. Outin, S. Gibot, P.E. Bollaert, Functional outcome of patients with prolonged hypoglycemic encephalopathy, Ann Intensive Care 7(1) (2017) 54.

[4] O. Albai, M. Frandes, R. Timar, D. Roman, B. Timar, Risk factors for developing dementia in type 2 diabetes mellitus patients with mild cognitive impairment, Neuropsychiatr Dis Treat 15 (2019) 167-175.

[5] S.S. Yun, J. Kim, S.J. Lee, J.S. So, M.Y. Lee, G. Lee, H.S. Lim, M. Kim, Naturally occurring benzoic, sorbic, and propionic acid in vegetables, Food Addit Contam Part B Surveill 12(3) (2019) 167-174.

[6] A. Filippone, M. Lanza, M. Campolo, G. Casili, I. Paterniti, S. Cuzzocrea, E. Esposito, The Anti-Inflammatory and Antioxidant Effects of Sodium Propionate, Int J Mol Sci 21(8) (2020).

[7] M. Luu, K. Weigand, F. Wedi, C. Breidenbend, H. Leister, S. Pautz, T. Adhikary, A. Visekruna, Regulation of the effector function of CD8(+) T cells by gut microbiota-derived metabolite butyrate, Sci Rep 8(1) (2018) 14430.

[8] S.U. Nurdin, R.K. Le Leu, G.P. Young, J.C. Stangoulis, C.T. Christophersen, C.A. Abbott, Analysis of the Anti-Cancer Effects of Cincau Extract (Premna oblongifolia Merr) and Other Types of Non-Digestible Fibre Using Faecal Fermentation Supernatants and Caco-2 Cells as a Model of the Human Colon, Nutrients 9(4) (2017).

[9] Y. Hu, D. Chen, B. Yu, H. Yan, P. Zheng, X. Mao, J. Yu, J. He, Z. Huang, Y. Luo, J. Luo, X. Zhang, L. Luo, Effects of dietary fibres on gut microbial metabolites and liver lipid metabolism in growing pigs, J Anim Physiol Anim Nutr (Berl) 104(5) (2020) 1484-1493.

[10] S. Park, J. Kang, S. Choi, H. Park, E. Hwang, Y.G. Kang, A.R. Kim, W. Holzapfel, Y. Ji, Cholesterol-lowering effect of Lactobacillus rhamnosus BFE5264 and its influence on the gut microbiome and propionate level in a murine model, PLoS One 13(8) (2018) e0203150.

[11] E.S. Chambers, A. Viardot, A. Psichas, D.J. Morrison, K.G. Murphy, S.E. Zac-Varghese, K. MacDougall, T. Preston, C. Tedford, G.S. Finlayson, J.E. Blundell, J.D. Bell, E.L. Thomas, S. Mt-Isa, D. Ashby, G.R. Gibson, S. Kolida, W.S. Dhillo, S.R. Bloom, W. Morley, S. Clegg, G. Frost, Effects of targeted delivery of propionate to the human colon on appetite regulation, body weight maintenance and adiposity in overweight adults, Gut 64(11) (2015) 1744-54.

[12] F. Ostendorf, J. Metzdorf, R. Gold, A. Haghikia, L. Tonges, Propionic Acid and Fasudil as Treatment Against Rotenone Toxicity in an In Vitro Model of Parkinson's Disease, Molecules 25(11) (2020).

[13] D. Bui, D. Ravasz, C. Chinopoulos, The Effect of 2-Ketobutyrate on Mitochondrial Substrate-Level Phosphorylation, Neurochem Res 44(10) (2019) 2301-2306.

[14] D. Liyanagamage, R.D. Martinus, Role of Mitochondrial Stress Protein HSP60 in Diabetes-Induced Neuroinflammation, Mediators Inflamm 2020 (2020) 8073516.

[15] K.A. Kim, Y.J. Shin, J.H. Kim, H. Lee, S.Y. Noh, S.H. Jang, O.N. Bae, Dysfunction of endothelial progenitor cells under diabetic conditions and its underlying mechanisms, Arch Pharm Res 35(2) (2012) 223-34.

bioRxiv preprint doi: https://doi.org/10.1101/2021.10.15.464493; this version posted October 16, 2021. The copyright holder for this preprint (which was not certified by peer review) is the author/funder. All rights reserved. No reuse allowed without permission.

[16] N.S. Dhalla, A.K. Shah, P.S. Tappia, Role of Oxidative Stress in Metabolic and Subcellular Abnormalities in Diabetic Cardiomyopathy, Int J Mol Sci 21(7) (2020).

[17] W. Nan, X. Zhonghang, C. Keyan, L. Tongtong, G. Wanshu, X. Zhongxin, Epigallocatechin-3-Gallate Reduces Neuronal Apoptosis in Rats after Middle Cerebral Artery Occlusion Injury via PI3K/AKT/eNOS Signaling Pathway, Biomed Res Int 2018 (2018) 6473580.

[18] J. Yang, The role of reactive oxygen species in angiogenesis and preventing tissue injury after brain ischemia, Microvasc Res 123 (2019) 62-67.

[19] Y. Yang, M.T. Torbey, Angiogenesis and Blood-Brain Barrier Permeability in Vascular Remodeling after Stroke, Curr Neuropharmacol 18(12) (2020) 1250-1265.

[20] A. Jambusaria, Z. Hong, L. Zhang, S. Srivastava, A. Jana, P.T. Toth, Y. Dai, A.B. Malik, J. Rehman, Endothelial heterogeneity across distinct vascular beds during homeostasis and inflammation, Elife 9 (2020).

[21] C. Wen, C. Huang, M. Yang, C. Fan, Q. Li, J. Zhao, D. Gan, A. Li, L. Zhu, D. Lu, The Secretion from Bone Marrow Mesenchymal Stem Cells Pretreated with Berberine Rescues Neurons with Oxidative Damage Through Activation of the Keap1-Nrf2-HO-1 Signaling Pathway, Neurotox Res 38(1) (2020) 59-73.

[22] P. Calcerrada, G. Peluffo, R. Radi, Nitric oxide-derived oxidants with a focus on peroxynitrite: molecular targets, cellular responses and therapeutic implications, Current pharmaceutical design 17(35) (2011) 3905-32.

[23] J.F. Tang, Q. Wen, J. Sun, W.M. Zhang, H.L. Zhu, Advances in the researches on the biological activities and inhibitors of phosphatidylinositol 3-kinase, Anti-cancer agents in medicinal chemistry 14(5) (2014) 673-87.

[24] F. Yang, Y. Zhang, Z. Tang, Y. Shan, X. Wu, H. Liu, Hemin treatment protects neonatal rats from sevoflurane-induced neurotoxicity via the phosphoinositide 3-kinase/Akt pathway, Life sciences 242 (2020) 117151.

[25] C. Dangelmaier, B.K. Manne, E. Liverani, J. Jin, P. Bray, S.P. Kunapuli, PDK1 selectively phosphorylates Thr(308) on Akt and contributes to human platelet functional responses, Thromb Haemost 111(3) (2014) 508-17.

[26] L. Xu, S. Wang, B. Li, A. Sun, Y. Zou, J. Ge, A protective role of ciglitazone in ox-LDL-induced rat microvascular endothelial cells via modulating PPARgamma-dependent AMPK/eNOS pathway, J Cell Mol Med 19(1) (2015) 92-102.

[27] M. Ishii, T. Nakahara, S. Ikeuchi, M. Nishimura, beta-Amyrin induces angiogenesis in vascular endothelial cells through the Akt/endothelial nitric oxide synthase signaling pathway, Biochem Biophys Res Commun 467(4) (2015) 676-82.

[28] J.H. Lee, A. Parveen, M.H. Do, Y. Lim, S.H. Shim, S.Y. Kim, Lespedeza cuneata protects the endothelial dysfunction via eNOS phosphorylation of PI3K/Akt signaling pathway in HUVECs, Phytomedicine 48 (2018) 1-9.

[29] R. Wang, G. Weng, S. Yu, S. Dai, W. Zhang, F. Zhu, Diffusion-weighted imaging detects early brain injury after hypothermic circulatory arrest in pigs, Interactive cardiovascular and thoracic surgery 26(4) (2018) 687-692.

[30] Y. An, Y. Kang, J. Lee, C. Ahn, K. Kwon, C. Choi, Blood flow characteristics of diabetic patients with complications detected by optical measurement, Biomed Eng Online 17(1) (2018) 25.

[31] A. Ahangarpour, A.A. Oroojan, L. Khorsandi, M. Kouchak, M. Badavi, Solid Lipid Nanoparticles of Myricitrin Have Antioxidant and Antidiabetic Effects on Streptozotocin-Nicotinamide-Induced

bioRxiv preprint doi: https://doi.org/10.1101/2021.10.15.464493; this version posted October 16, 2021. The copyright holder for this preprint (which was not certified by peer review) is the author/funder. All rights reserved. No reuse allowed without permission.

Diabetic Model and Myotube Cell of Male Mouse, Oxidative medicine and cellular longevity 2018 (2018) 7496936.

[32] Y. Zeng, X. Wang, B. Yin, G. Xia, Z. Shen, W. Gu, M. Wu, Role of the stromal cell derived factor-1/CXC chemokine receptor 4 axis in the invasion and metastasis of lung cancer and mechanism, Journal of thoracic disease 9(12) (2017) 4947-4959.

[33] N.V. Sayapina, A.A. Sergievich, V.L. Kuznetsov, V.V. Chaika, I.G. Lisitskaya, P.P. Khoroshikh, T.A. Batalova, K. Tsarouhas, D. Spandidos, A.M. Tsatsakis, C. Fenga, K.S. Golokhvast, Influence of multi-walled carbon nanotubes on the cognitive abilities of Wistar rats, Experimental and therapeutic medicine 12(3) (2016) 1311-1318.

[34] J.F. Cryan, C. Mombereau, In search of a depressed mouse: utility of models for studying depression-related behavior in genetically modified mice, Mol Psychiatry 9(4) (2004) 326-57.

[35] S. Ide, T. Takahashi, Y. Takamatsu, G.R. Uhl, H. Niki, I. Sora, K. Ikeda, Distinct Roles of Opioid and Dopamine Systems in Lateral Hypothalamic Intracranial Self-Stimulation, The international journal of neuropsychopharmacology 20(5) (2017) 403-409.

[36] R. Yankelevitch-Yahav, M. Franko, A. Huly, R. Doron, The forced swim test as a model of depressive-like behavior, J Vis Exp (97) (2015).

[37] M.S. Stieglitz, S. Fenske, V. Hammelmann, E. Becirovic, V. Schöttle, J.E. Delorme, M. Schöll-Weidinger, R. Mader, J. Deussing, D.P. Wolfer, M.W. Seeliger, U. Albrecht, C.T. Wotjak, M. Biel, S. Michalakis, C. Wahl-Schott, Disturbed Processing of Contextual Information in HCN3 Channel Deficient Mice, Frontiers in molecular neuroscience 10 (2017) 436.

[38] W.M. Arika, C.M. Kibiti, J.M. Njagi, M.P. Ngugi, Modulation of Cognition: The Role of Gnidia glauca on Spatial Learning and Memory Retention in High-Fat Diet-Induced Obese Rats, Neural plasticity 2019 (2019) 2867058.

[39] A. Poznyak, A.V. Grechko, P. Poggio, V.A. Myasoedova, V. Alfieri, A.N. Orekhov, The Diabetes Mellitus-Atherosclerosis Connection: The Role of Lipid and Glucose Metabolism and Chronic Inflammation, Int J Mol Sci 21(5) (2020).

[40] H. Umegaki, Therapeutic Potential of Antidiabetic Medications in the Treatment of Cognitive Dysfunction and Dementia, Drugs & aging 33(6) (2016) 399-409.

[41] S. Wang, S.L. Zhou, F.Y. Min, J.J. Ma, X.J. Shi, E. Bereczki, J. Wu, mTOR-mediated hyperphosphorylation of tau in the hippocampus is involved in cognitive deficits in streptozotocin-induced diabetic mice, Metabolic brain disease 29(3) (2014) 729-36.

[42] J. Kim, S.H. Shin, J.K. Kang, J.W. Kim, HX-1171 attenuates pancreatic β-cell apoptosis and hyperglycemia-mediated oxidative stress via Nrf2 activation in streptozotocin-induced diabetic model, Oncotarget 9(36) (2018) 24260-24271.

[43] C. Brufani, D. Fintini, V. Nobili, P.I. Patera, M. Cappa, M. Brufani, Use of metformin in pediatric age, Pediatr Diabetes 12(6) (2011) 580-8.

[44] I. Thomas, B. Gregg, Metformin; a review of its history and future: from lilac to longevity, Pediatr Diabetes 18(1) (2017) 10-16.

[45] Z. Lv, Y. Guo, Metformin and Its Benefits for Various Diseases, Front Endocrinol (Lausanne) 11 (2020) 191.

[46] I. Gantois, A. Khoutorsky, J. Popic, A. Aguilar-Valles, E. Freemantle, R. Cao, V. Sharma, T. Pooters, A. Nagpal, A. Skalecka, V.T. Truong, S. Wiebe, I.A. Groves, S.M. Jafarnejad, C. Chapat, E.A. McCullagh, K. Gamache, K. Nader, J.C. Lacaille, C.G. Gkogkas, N. Sonenberg, Metformin ameliorates core deficits in a mouse model of fragile X syndrome, Nat Med 23(6) (2017) 674-677.

bioRxiv preprint doi: https://doi.org/10.1101/2021.10.15.464493; this version posted October 16, 2021. The copyright holder for this preprint (which was not certified by peer review) is the author/funder. All rights reserved. No reuse allowed without permission.

[47] H.K. Greger, L.G.E. Hanem, H.F. Ostgard, E. Vanky, Cognitive function in metformin exposed children, born to mothers with PCOS - follow-up of an RCT, BMC Pediatr 20(1) (2020) 60.

[48] A.A. Soukas, H. Hao, L. Wu, Metformin as Anti-Aging Therapy: Is It for Everyone?, Trends Endocrinol Metab 30(10) (2019) 745-755.

[49] Y.C. Huang, C.C. Hsu, W.C. Lin, T.K. Yin, C.W. Huang, P.W. Wang, H.H. Chang, N.T. Chiu, Effects of metformin on the cerebral metabolic changes in type 2 diabetic patients, ScientificWorldJournal 2014 (2014) 694326.

[50] R.A. Wimmer, A. Leopoldi, M. Aichinger, N. Wick, B. Hantusch, M. Novatchkova, J. Taubenschmid, M. Hämmerle, C. Esk, J.A. Bagley, D. Lindenhofer, G. Chen, M. Boehm, C.A. Agu, F. Yang, B. Fu, J. Zuber, J.A. Knoblich, D. Kerjaschki, J.M. Penninger, Human blood vessel organoids as a model of diabetic vasculopathy, Nature 565(7740) (2019) 505-510.

[51] J.Y. Huang, L.T. Li, H. Wang, S.S. Liu, Y.M. Lu, M.H. Liao, R.R. Tao, L.J. Hong, K. Fukunaga, Z. Chen, C.S. Wilcox, E.Y. Lai, F. Han, In vivo two-photon fluorescence microscopy reveals disturbed cerebral capillary blood flow and increased susceptibility to ischemic insults in diabetic mice, CNS Neurosci Ther 20(9) (2014) 816-22.

[52] S. Ogoh, Relationship between cognitive function and regulation of cerebral blood flow, The journal of physiological sciences : JPS 67(3) (2017) 345-351.

[53] S. Zhang, R. Xue, R. Hu, The neuroprotective effect and action mechanism of polyphenols in diabetes mellitus-related cognitive dysfunction, European journal of nutrition 59(4) (2020) 1295-1311.

[54] P.B. Bagatini, L.L. Xavier, K. Bertoldi, F. Moysés, G. Lovatel, L.T. Neves, S. Barbosa, L. Saur, P.N. de Senna, A.A. Souto, I.R. Siqueira, M. Achaval, An evaluation of aversive memory and hippocampal oxidative status in streptozotocin-induced diabetic rats treated with resveratrol, Neuroscience letters 636 (2017) 184-189.

[55] D. Dymkowska, B. Drabarek, P. Podszywałow-Bartnicka, J. Szczepanowska, K. Zabłocki, Hyperglycaemia modifies energy metabolism and reactive oxygen species formation in endothelial cells in vitro, Archives of biochemistry and biophysics 542 (2014) 7-13.

[56] P. Karki, K.G. Birukov, Rho and Reactive Oxygen Species at Crossroads of Endothelial Permeability and Inflammation, Antioxidants & redox signaling 31(13) (2019) 1009-1022.

bioRxiv preprint doi: https://doi.org/10.1101/2021.10.15.464493; this version posted October 16, 2021. The copyright holder for this preprint (which was not certified by peer review) is the author/funder. All rights reserved. No reuse allowed without permission.

Tables

Table 1

Blood glucose in the IPGTT test.

Groups	Time (min)			
	0	30	60	120
Ctrl	5.9±0.74	8.5±0.93	7.6±1.09	5.4±0.63
STZ	21.7±3.35###	25.6±4.22###	22.7±4.45###	20.7±4.40###
STZ+Pro-37.5	17.8±5.14	19.7±4.59**	18.8±3.88	16.4+2.54*
STZ+Pro-75	11.5±3.37***	14.5±3.43***	12.5±3.21***	10.4±3.53***
STZ+Pro-150	18.7±4.09	20.2±4.28*	18.9±4.93	16.8±4.05
STZ+Met	12.4±2.57***	15.1±3.44***	11.7±2.42***	9.5±2.68***

Data were expressed as mean ± SD (N = 10). ###p < 0.001 vs. Ctrl group, *p < 0.05, **p < 0.01, and ***p < 0.001 vs. STZ group.

Table 2

The exact escape latency in morris water maze values in seconds.

Groups	Escape latency (sec)			
	Day1	Day2	Day3	Day4
Ctrl	54.9±5.31	46.5±7.08	37.7±2.64	27.1±2.91
STZ	58.7±2.05	57.3±3.38$^{\#}$	51.0±5.48$^{\#\#}$	44.7±4.17$^{\#\#\#}$
STZ + Pro-75	52.8±7.87	45.7±4.43**	35.9±4.98**$^{,\$}$	25.7±2.59***$^{,\$\$}$
STZ + Met	53.6±7.59	48.8±3.11**	46.4±7.43	36.0±5.51*

Data were expressed as mean ± SD (N = 10). #p < 0.05, ##p < 0.01, and ###p < 0.001 vs. Ctrl group, *p < 0.05, **p < 0.01, and ***p < 0.001 vs. STZ group, $^{\$}$p < 0.05 and $^{\$\$}$p < 0.01 vs. STZ + Met group.

bioRxiv preprint doi: https://doi.org/10.1101/2021.10.15.464493; this version posted October 16, 2021. The copyright holder for this preprint (which was not certified by peer review) is the author/funder. All rights reserved. No reuse allowed without permission.

Figure legends

Fig. 1 Diagram illustrating the designing of the research, with drug administration included, neuro-behavior related evaluation, histology-related evaluation, biochemistry-related analyzing as well as protein expressing processes.

Fig. 2. Effects of propionate on FBG and IPGTT. (A) FBG levels; (B) IPGTT test 36 days after STZ induction. (B) The AUC of blood glucose in the IPGTT test. The data are expressed as the mean ± SD (N = 10). $^{###}$p < 0.001 vs Ctrl group; *p < 0.05, **p < 0.01 and ***p < 0.001 vs STZ group.

Fig. 3. The body weight data of the untreated control group, the streptozotocin exposure group, and the groups treated with propionate and metformin. All data were expressed as mean ± SD (N = 10). $^{###}$p < 0.001 vs Ctrl group; **p < 0.01 and ***p < 0.001 vs STZ group.

Fig. 4. The effect of propionate on LCBF in mouse cerebral cortex. (A) Representative images of LCBF in different groups. The magnitude of LCBF is represented by different colors, with blue to red indicating low to high. (B) Quantitative analysis of LCBF in all groups. Data were expressed as mean ± SD (n = 6). ###p < 0.001 vs. Ctrl group, **p < 0.01 vs. STZ group, n.s., no significant difference.

Fig. 5. Levels of oxidative stress. (A and B) STZ decreased CAT and SOD. Pretreatment with propionate attenuated these decrements. (C and D) STZ increased MDA and ROS levels in mice brains. Pretreatment with propionate attenuated these increments. Data were expressed as mean ± SD (n = 6). ###p < 0.001 and ##p < 0.01 vs. Ctrl group, *p < 0.05 and **p < 0.01 vs. STZ group, $^{\$}$p < 0.05 vs. STZ + Met group, n.s., no significant difference.

Fig. 6. Effects of propionate on ATP level and NO release in brain tissues. Data were expressed as mean ± SD (N = 6). #p < 0.05 and ###p < 0.001 vs. Ctrl group, *p < 0.05, **p < 0.01 and ***p < 0.001 vs. STZ group, $^{\$}$p < 0.05 vs. STZ + Met group. n.s., no significant difference.

Fig. 7. Cellular structures in the hippocampus are visible after Nissl staining. (A-D) Representation images of Ctrl, STZ, STZ + Pro, and STZ + Met, 36 days after T1D induction. (E) Quantitative of neurons in the CA3. The red arrows indicate normal neurons, while the black arrows indicate necrosis neurons. Scale bar = 100 μm. Data were expressed as mean ± SD (N = 3). ###p < 0.001 vs. Ctrl group, ***p < 0.001 vs. STZ group, $^{\$\$}$p < 0.01 vs. STZ + Met group.

Fig. 8. Animal behavior analysis in the open field test. In the OFT, the travel distance (A), number of standing (B), time spent at the center (C) and immobility time (D) were recorded and analyzed. Data were expressed as mean ± SD (N = 10). #p < 0.05 and ###p < 0.001 vs. Ctrl group, *p < 0.05 and ***p < 0.001 vs. STZ group, $^{\$}$p < 0.05 vs. STZ + Met group, n.s., no significant difference.

Fig. 9. Results of elevated plus maze test. Open arms entry times (A) and retention time in open arms (B) were recorded and analyzed. Data were expressed as mean ± SD (N = 10). #p < 0.05 and ##p < 0.01 vs. Ctrl group, *p < 0.05 vs. STZ group, $^{\$}$p < 0.05 vs. STZ + Met group, n.s., no significant difference.

Fig. 10. The influence of propionate on STZ-induced depression-like behavior evaluated by tail suspension test (TST) and force swimming test (FST). Quiescent time in TST (A), number of climbing times (B), and immobility time in FST (C) were measured and analyzed. Data were expressed as mean ± SD (N = 10). #p < 0.05 and ###p < 0.001 vs. Ctrl group, *p < 0.05, **p < 0.01, ***p < 0.001 vs. STZ group, $^{\$}$p < 0.05 vs. STZ + Met group, n.s., no significant difference.

Fig. 11. Escape latencies are shown as the mean value of each trail session for four sequential days (A). Swimming tracks are recorded via a video tracking camera system (B).

bioRxiv preprint doi: https://doi.org/10.1101/2021.10.15.464493; this version posted October 16, 2021. The copyright holder for this preprint (which was not certified by peer review) is the author/funder. All rights reserved. No reuse allowed without permission.

Fig. 12. Influence of propionate on STZ-induced cognition and memory dysfunction measured by MWM test. Crossing into the former location of the platform (A), time spent in the target quadrant in probe task (B) and Swimming speed (C) were recorded and analyzed. Data were expressed as mean ± SD (N = 10). #$p < 0.05$ and ##$p < 0.01$ vs. Ctrl group, *$p < 0.05$, **$p < 0.01$, and ***$p < 0.001$ vs. STZ group, $^{\$}p < 0.05$ vs. STZ + Met group, n.s., no significant difference.

Fig. 13. Phosphorylation of PI3K/AKT/eNOS signaling pathway proteins, as measured by western blotting. Representative western blot images (A) and the ratio of p-PI3K/PI3K (B), p-AKT/AKT (C), and p-eNOS/eNOS. GAPDH served as an internal control. Data are presented as the mean ± standard deviation (n=3 independent experiments). #$p < 0.05$ vs. Ctrl group, *$p < 0.05$ and ***$p < 0.001$ vs. STZ group, $^{\$}p < 0.05$ vs. STZ + Met group, n.s., no significant difference.

bioRxiv preprint doi: https://doi.org/10.1101/2021.10.15.464493; this version posted October 16, 2021. The copyright holder for this preprint (which was not certified by peer review) is the author/funder. All rights reserved. No reuse allowed without permission.

Figures

Fig. 1

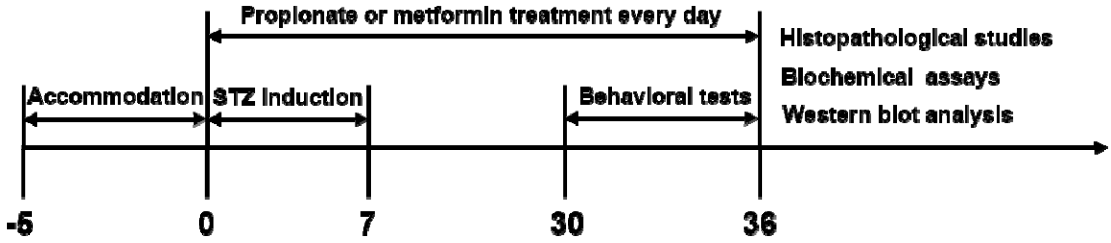

Fig. 2

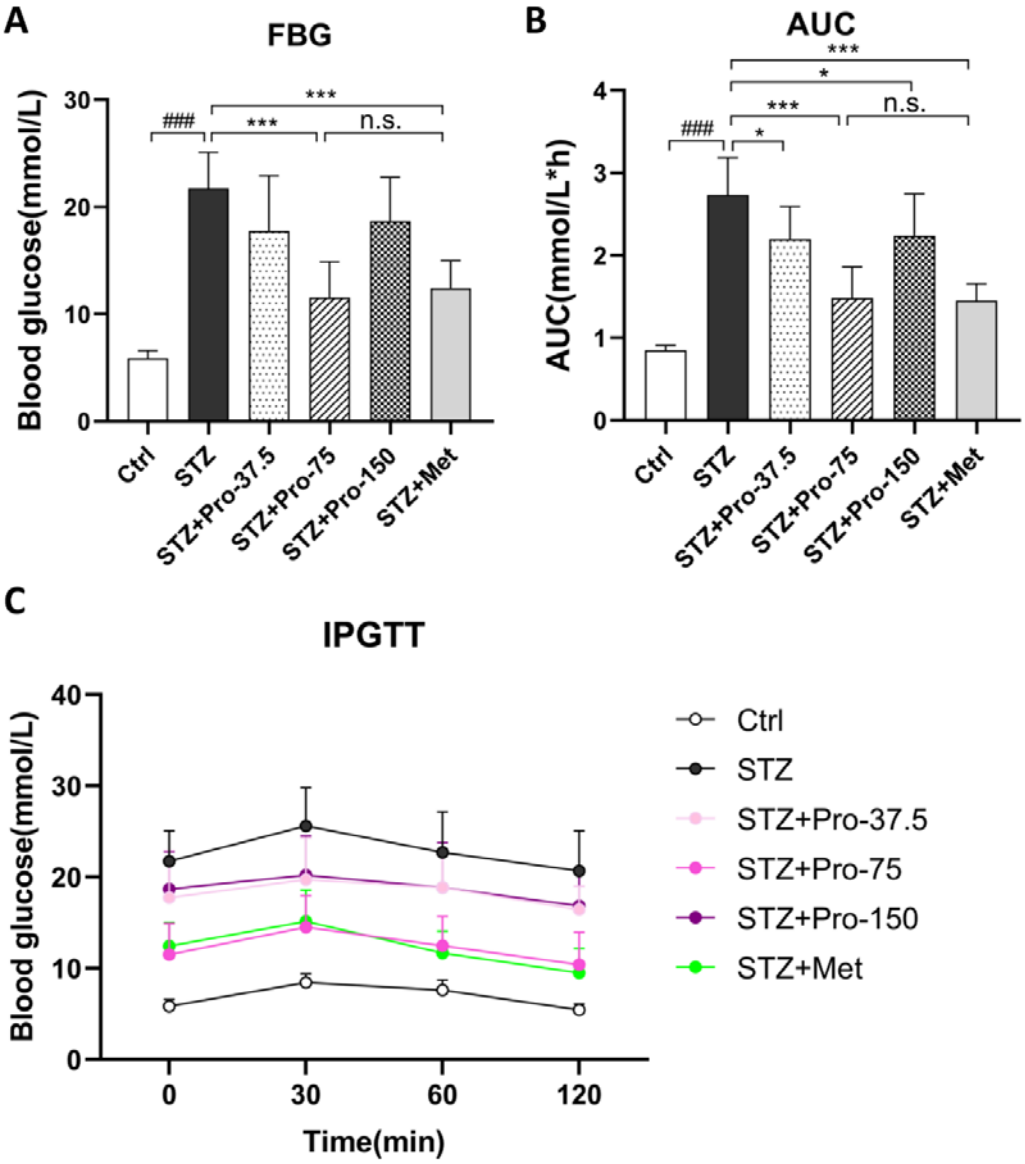

Fig. 3

bioRxiv preprint doi: https://doi.org/10.1101/2021.10.15.464493; this version posted October 16, 2021. The copyright holder for this preprint (which was not certified by peer review) is the author/funder. All rights reserved. No reuse allowed without permission.

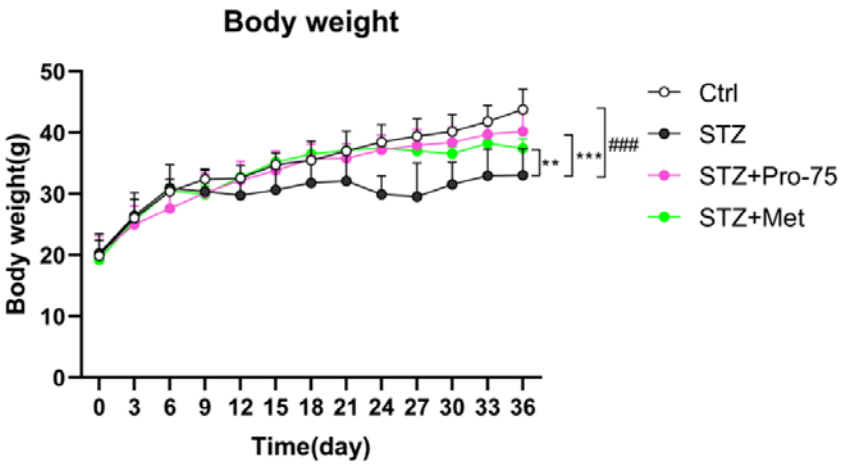

Fig. 4

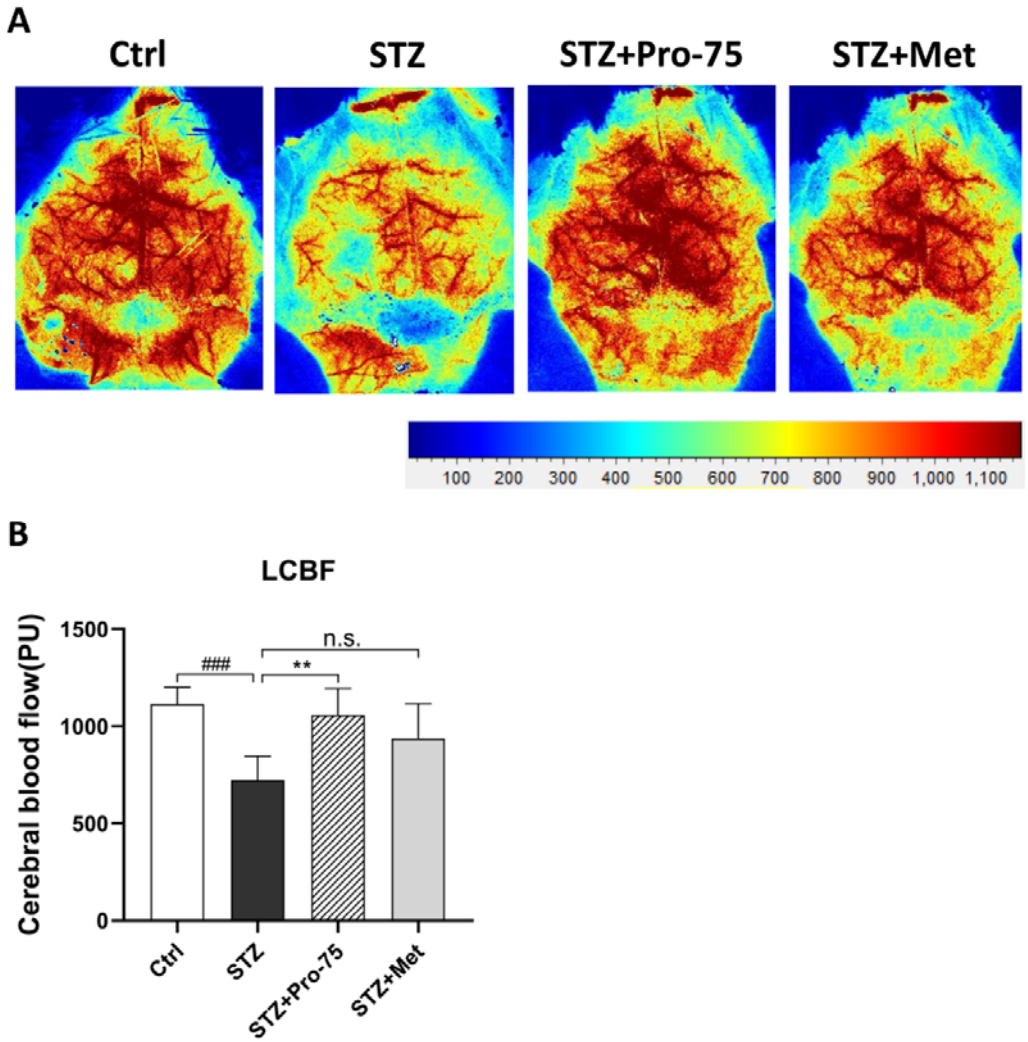

Fig. 5

bioRxiv preprint doi: https://doi.org/10.1101/2021.10.15.464493; this version posted October 16, 2021. The copyright holder for this preprint (which was not certified by peer review) is the author/funder. All rights reserved. No reuse allowed without permission.

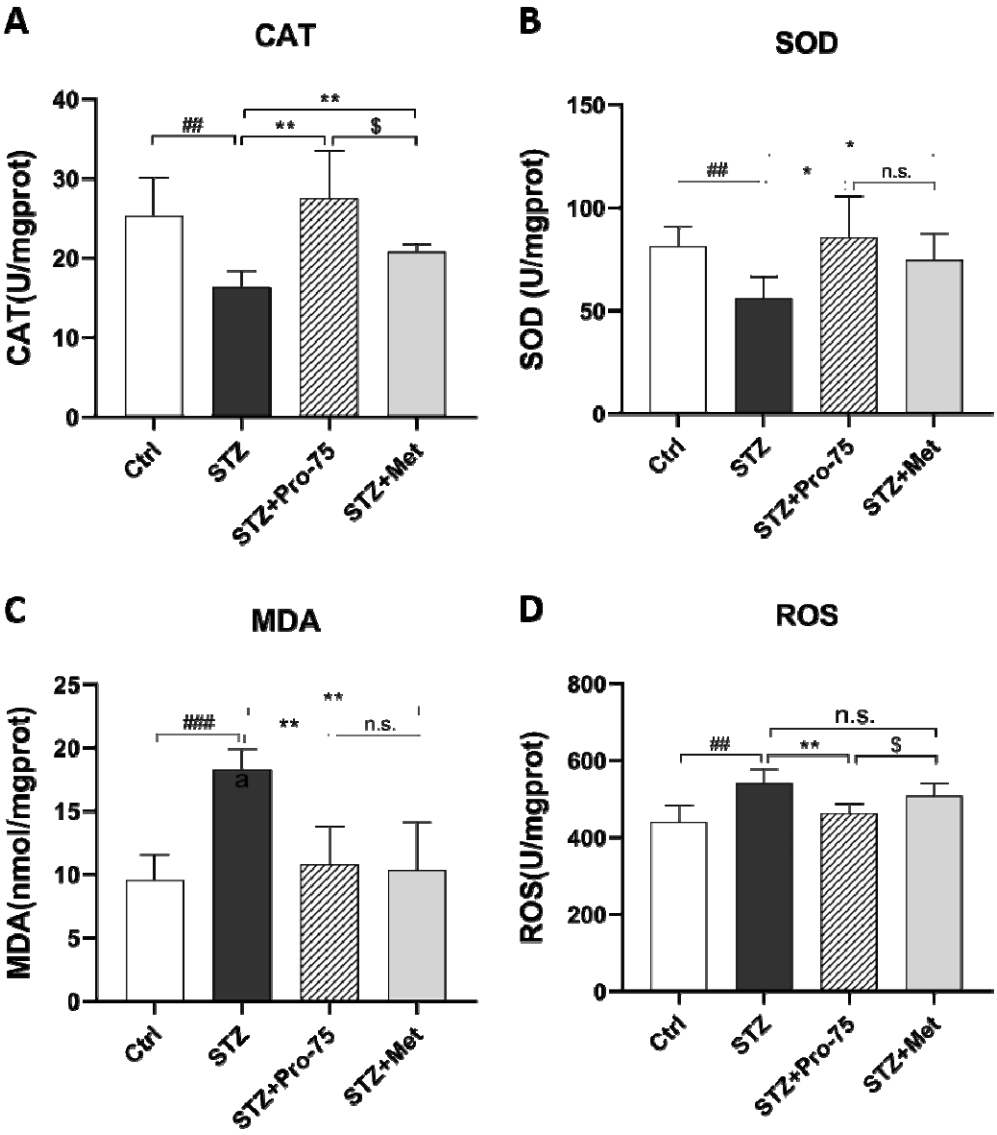

Fig. 6

bioRxiv preprint doi: https://doi.org/10.1101/2021.10.15.464493; this version posted October 16, 2021. The copyright holder for this preprint (which was not certified by peer review) is the author/funder. All rights reserved. No reuse allowed without permission.

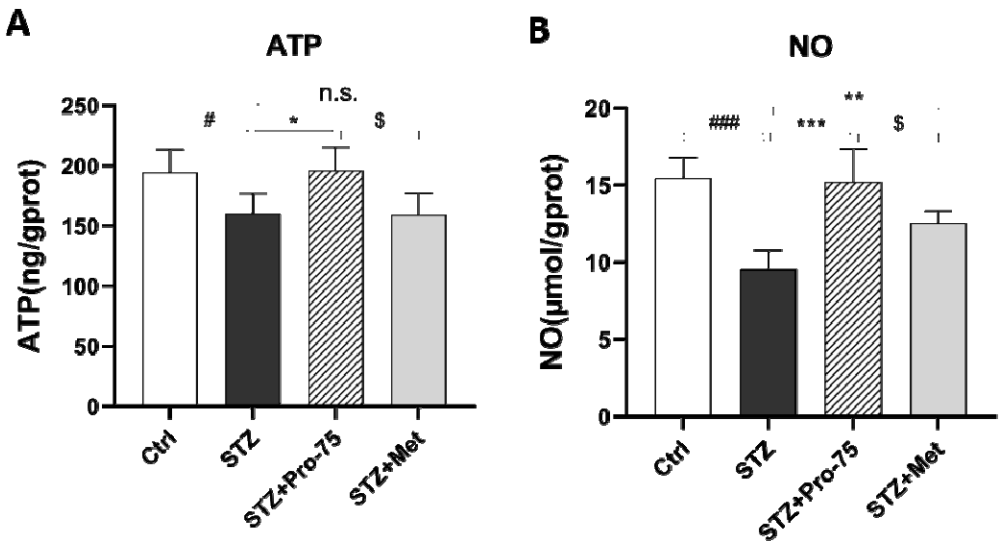

Fig. 7

bioRxiv preprint doi: https://doi.org/10.1101/2021.10.15.464493; this version posted October 16, 2021. The copyright holder for this preprint (which was not certified by peer review) is the author/funder. All rights reserved. No reuse allowed without permission.

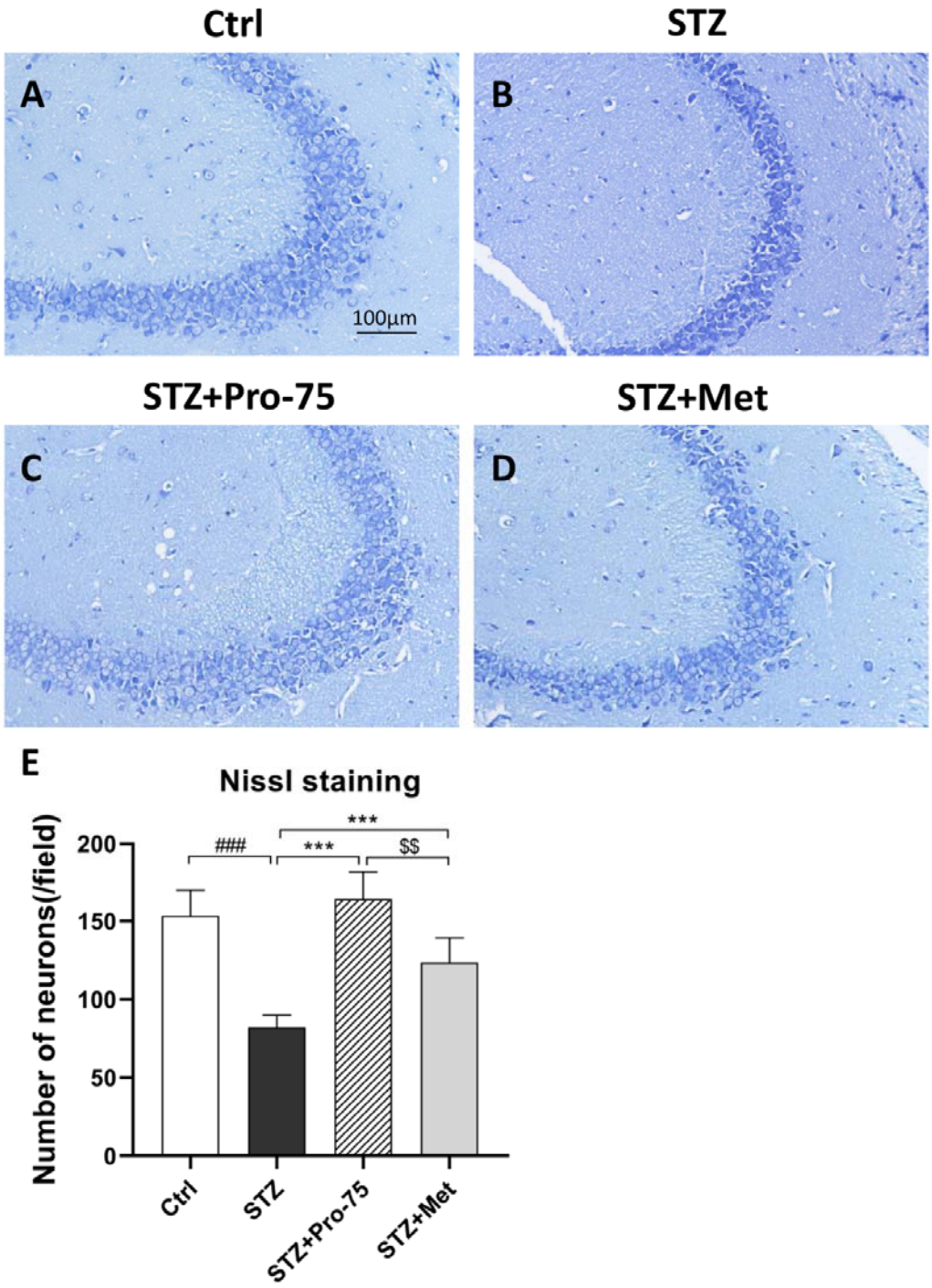

Fig. 8

bioRxiv preprint doi: https://doi.org/10.1101/2021.10.15.464493; this version posted October 16, 2021. The copyright holder for this preprint (which was not certified by peer review) is the author/funder. All rights reserved. No reuse allowed without permission.

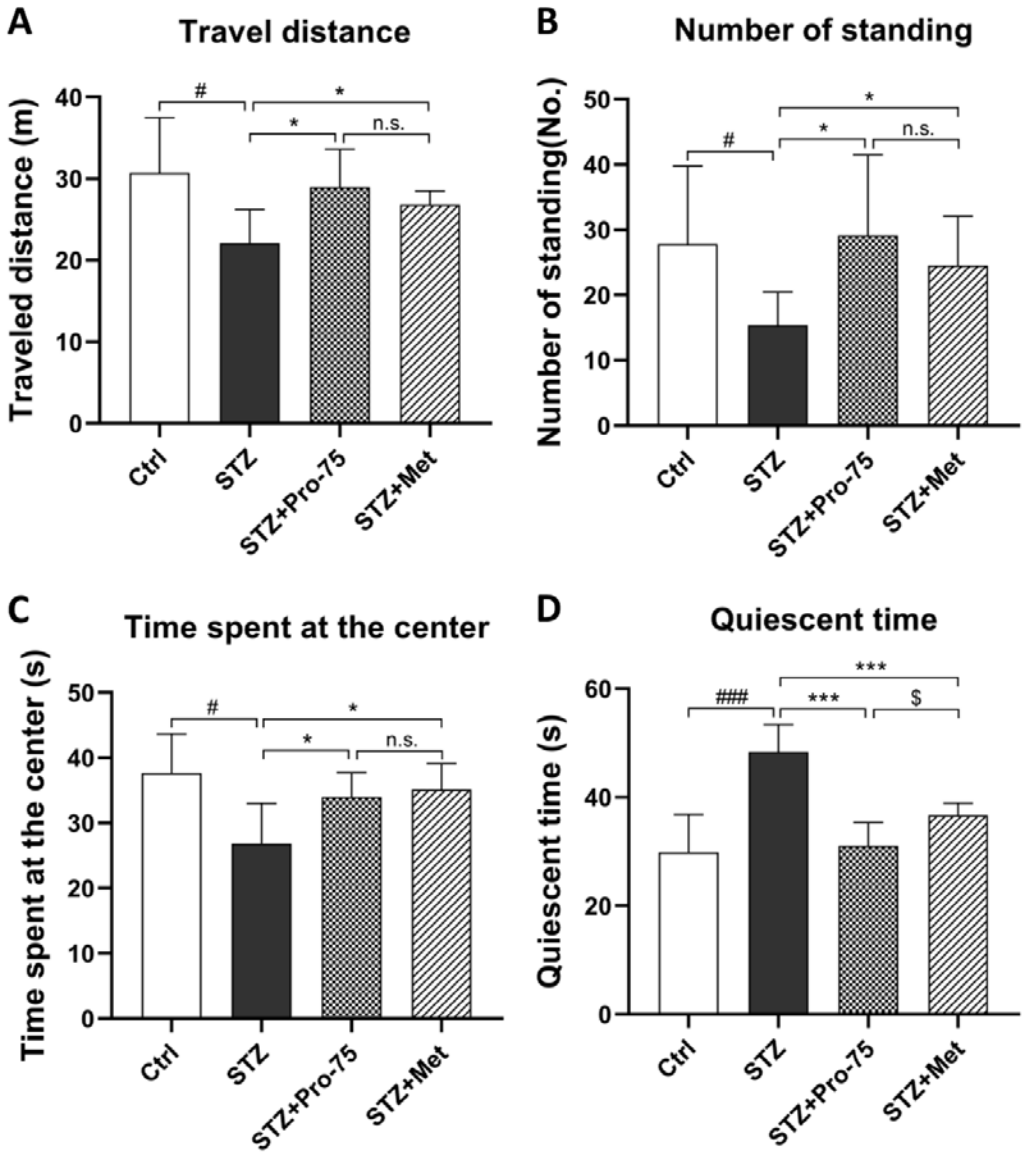

Fig. 9

bioRxiv preprint doi: https://doi.org/10.1101/2021.10.15.464493; this version posted October 16, 2021. The copyright holder for this preprint (which was not certified by peer review) is the author/funder. All rights reserved. No reuse allowed without permission.

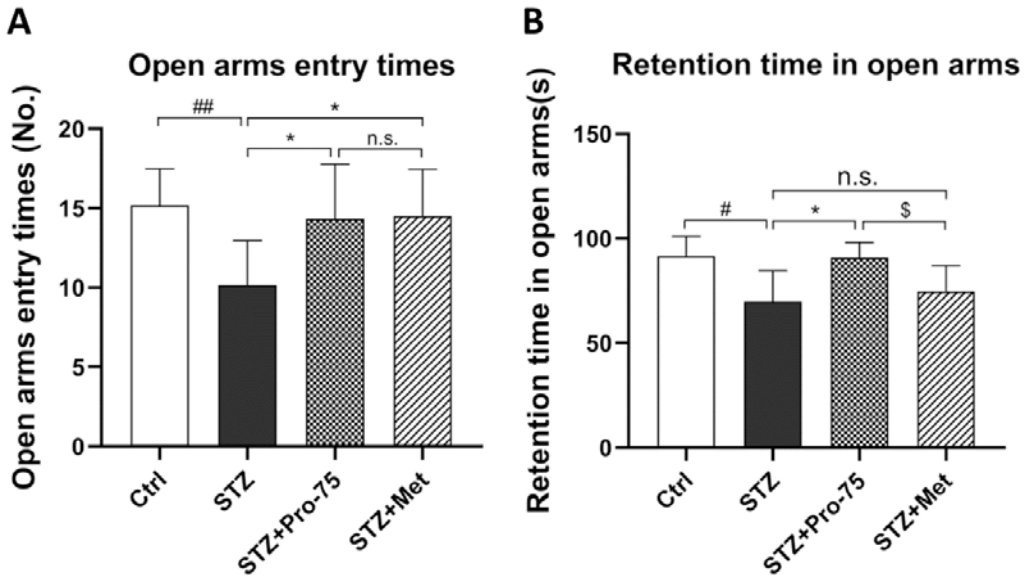

Fig. 10

bioRxiv preprint doi: https://doi.org/10.1101/2021.10.15.464493; this version posted October 16, 2021. The copyright holder for this preprint (which was not certified by peer review) is the author/funder. All rights reserved. No reuse allowed without permission.

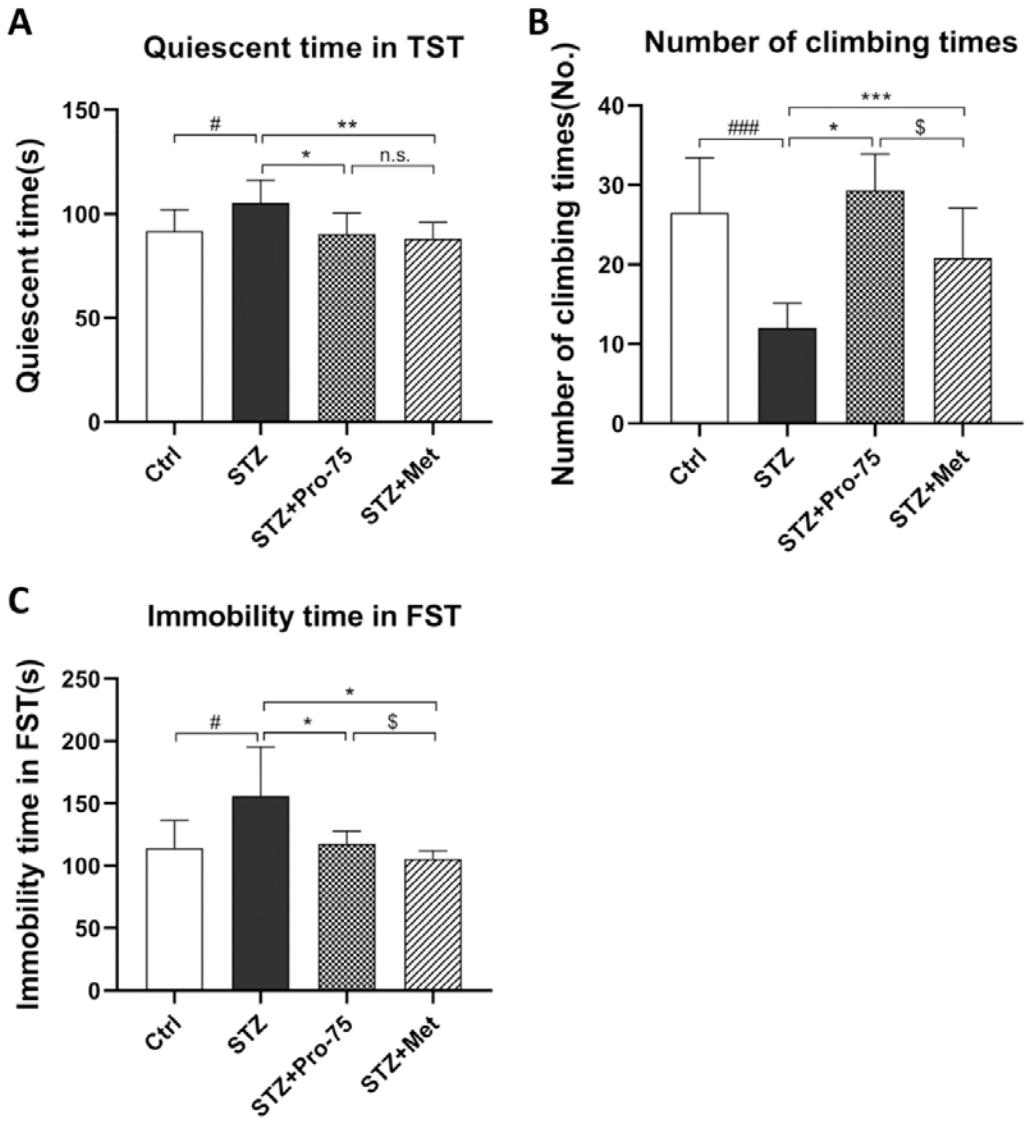

Fig. 11

bioRxiv preprint doi: https://doi.org/10.1101/2021.10.15.464493; this version posted October 16, 2021. The copyright holder for this preprint (which was not certified by peer review) is the author/funder. All rights reserved. No reuse allowed without permission.

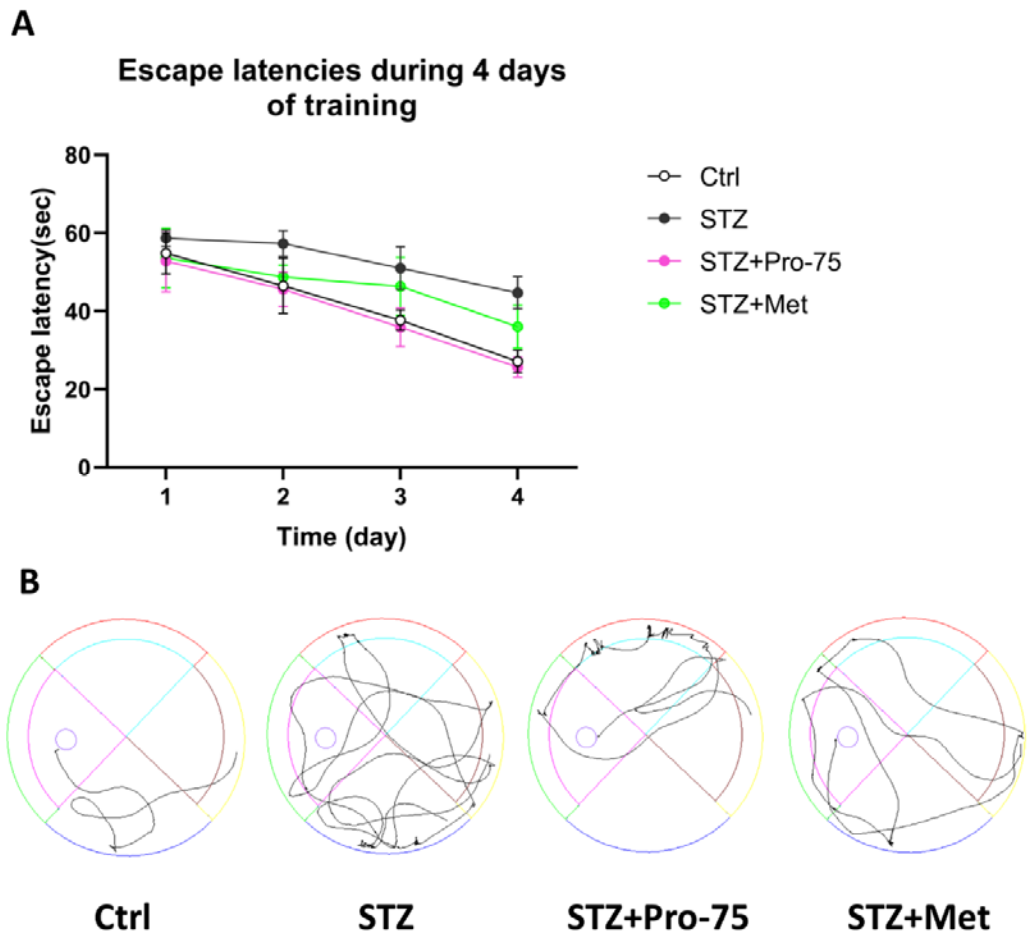

Fig. 12

bioRxiv preprint doi: https://doi.org/10.1101/2021.10.15.464493; this version posted October 16, 2021. The copyright holder for this preprint (which was not certified by peer review) is the author/funder. All rights reserved. No reuse allowed without permission.

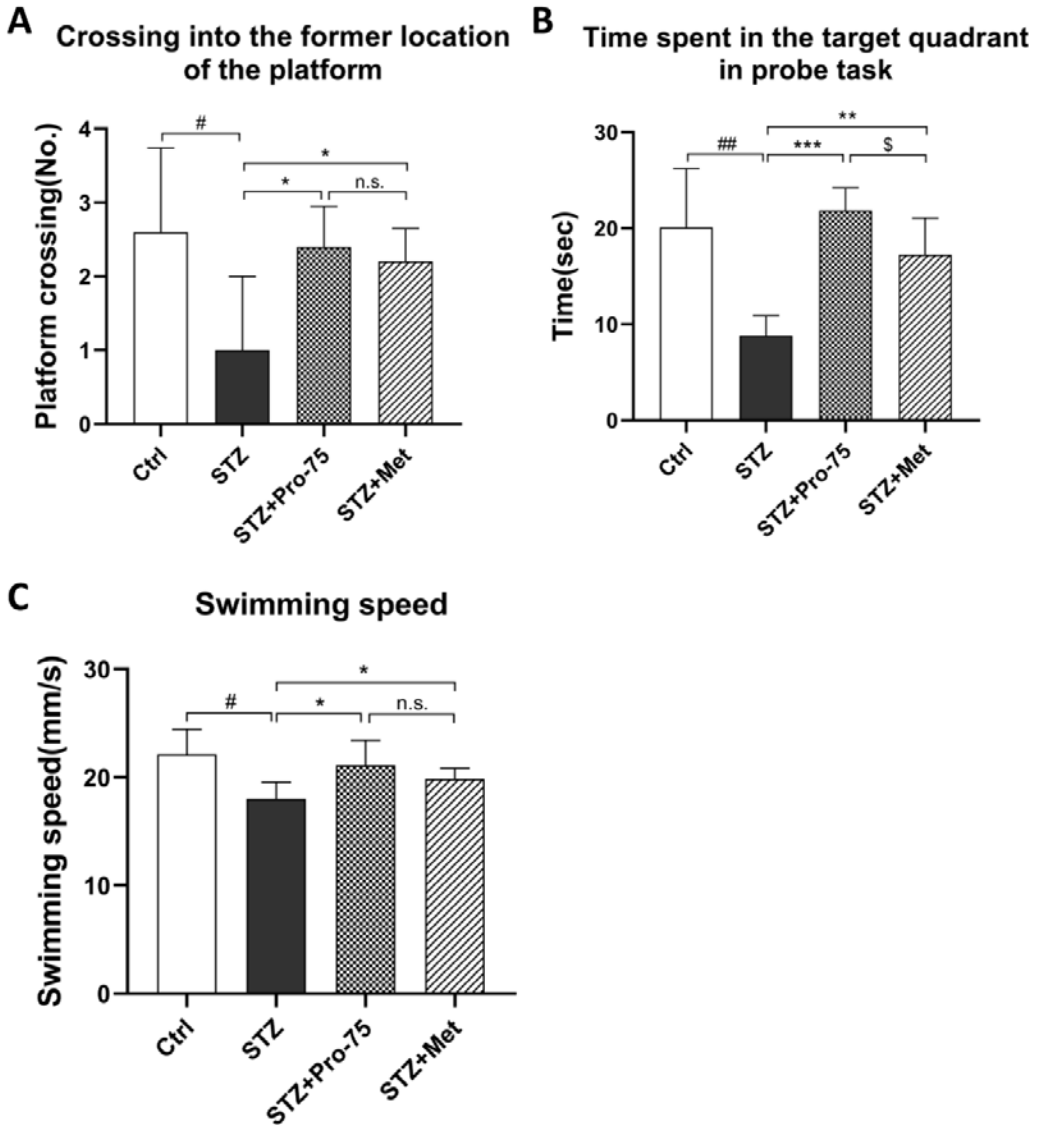

Fig. 13
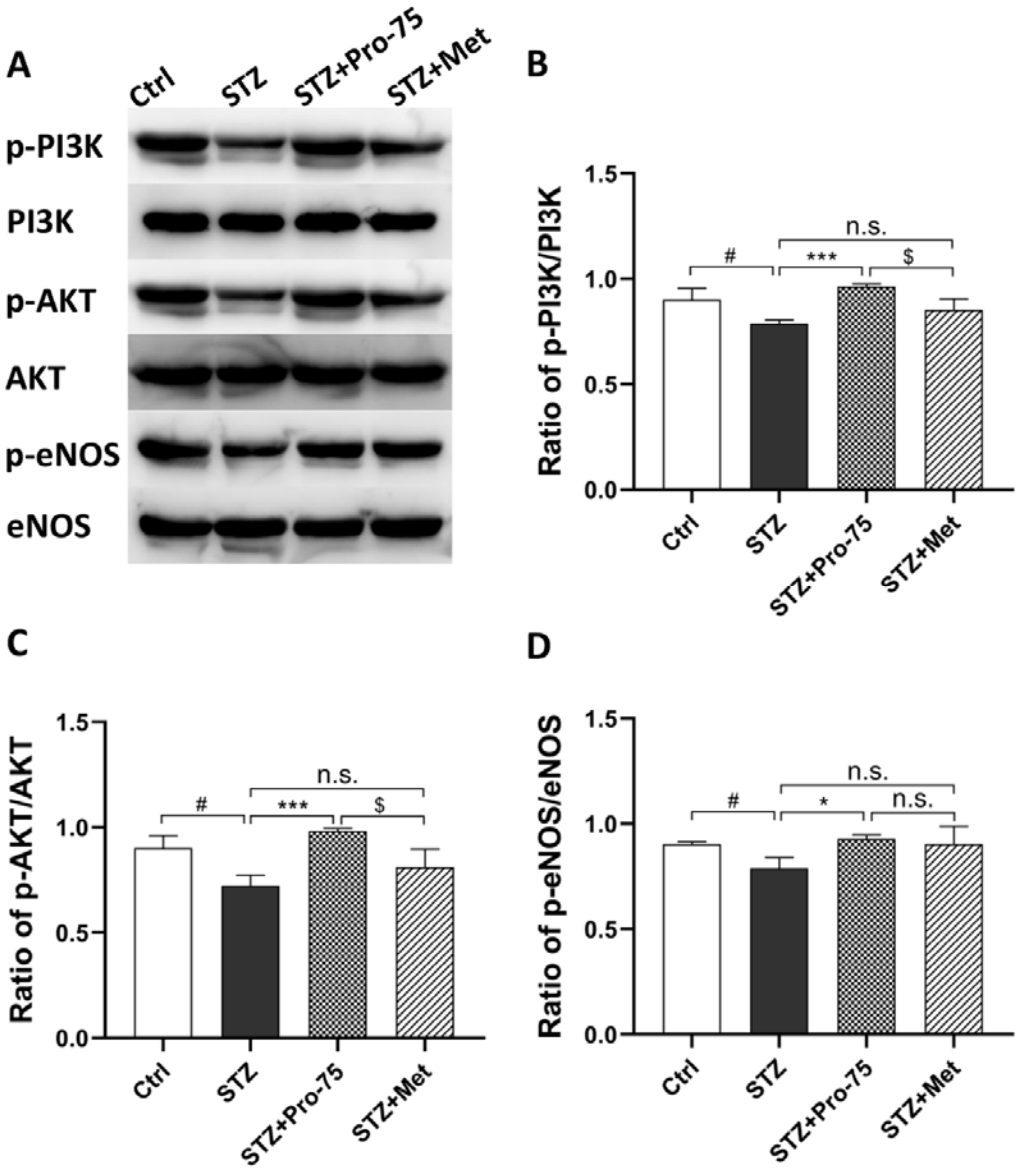
bioRxiv preprint doi: https://doi.org/10.1101/2021.10.15.464493; this version posted October 16, 2021. The copyright holder for this preprint (which was not certified by peer review) is the author/funder. All rights reserved. No reuse allowed without permission.